2012

Vibration Reduction of Offshore Wind Turbines Using Tuned Liquid Column Dampers

Colin Roderick
University of Massachusetts Amherst, crode0@engin.umass.edu

VIBRATION REDUCTION OF OFFSHORE WIND TURBINES USING TUNED LIQUID COLUMN DAMPERS

A Thesis Presented

by

COLIN RODERICK

Submitted to the Graduate School of the
University of Massachusetts Amherst in partial fulfillment
of the requirements for the degree of

MASTER OF SCIENCE IN MECHANICAL ENGINEERING

September 2012

Mechanical Engineering

VIBRATION REDUCTION OF OFFSHORE WIND TURBINES USING TUNED LIQUID COLUMN DAMPERS

A Thesis Presented

by

COLIN RODERICK

Approved as to style and content by:

_____

Matthew Lackner, Chair

_____

Sanjay Arwade, Member

_____

James Manwell, Member

_____

David Schmidt, Graduate Program Director
Department of Mechanical and Industrial Engineering

ABSTRACT

VIBRATION REDUCTION OF OFFSHORE WIND TURBINES USING TUNED LIQUID COLUMN DAMPERS

SEPTEMBER 2012

COLIN RODERICK
B.S.E, ROGER WILLIAMS UNIVERSITY
M.S.M.E., UNIVERSITY OF MASSACHUSETTS AMHERST
Directed by: Professor Matthew Lackner

Wind turbines are becoming an accepted method for generating electricity. With technology advancements and mapping of the global wind resource, offshore locations are now utilized for turbine placement due to their strong and consistent winds. Though these offshore areas offer high power density values, the environmental conditions in these locations often impose high wind and wave forces on offshore wind turbines (OWTs) making them susceptible to intense loading and undesirable vibrations. It has therefore become necessary to utilize mechanical techniques for making OWTs more adapted to external conditions. One method to reduce system vibrations is through the use of structural control devices typically utilized in civil structures. Among the many types of structural control devices, tuned liquid column dampers (TLCDs) show great promise in the application to OWTs due to their high performance and low cost. This thesis examines the use of TLCDs in a monopile as well as floating barge and spar buoy OWTs.

Equations of motion for limited degree-of-freedom TLCD-turbine models are presented. A baseline analysis of each OWT is performed to generate a quantitative comparison to show how a TLCD would affect the overall dynamics of the system. The

models are then subjected to two methods of testing. The first is an initial perturbation method where the tower is displaced and allowed to oscillate according to the structural and environmental conditions. The second method subjects the system to realistic wind and wave thrusting functions. Optimal TLCD dimensions are derived for the models using a deterministic sweep method. The TLCD configurations examined include those with a uniform and non-uniform column cross-sectional area. In most cases, the TLCD is shown to successfully reduce overall tower top displacement of each of the OWTs as well as the platform pitch when applicable. In some cases, use of the TLCD actually increases overall tower and platform motion.

This thesis also examines the use of idealized tuned mass dampers (TMDs) in OWTs when utilized in the modified aero-elastic code, FAST-SC. Comparisons between the optimized TLCD and the idealized TMD are made with regards to motion reduction and damper parameter values.

TABLE OF CONTENTS

Page

LIST OF TABLES

Table **Page**

LIST OF FIGURES

CHAPTER 1

INTRODUCTION

1.1 Background and Motivation

With increasing energy demands and the depletion of the earth's fossil fuels, wind turbines have become a viable and cost-effective means for producing electricity. Wind energy development can offset fossil fuel usage and impact the global energy portfolio. Offshore locations offer outstanding wind conditions for wind turbine energy generation because of high and consistent wind speeds, lower intrinsic turbulence intensities, and low shear [20]. These conditions result in significantly increased turbine capacity factors compared to onshore locations [11]. Although the wind resource is advantageous, developing offshore wind energy also presents a number of challenges. As technology has progressed over the years, offshore wind turbines (OWTs) have become larger in size and are being placed in deeper waters. OWTs will subsequently be subjected to harsher external conditions including high wind, wave, current, and possibly ice forces. This results in increased system-wide dynamic loading on the structures. These forces create undesirable vibrations in the structure, which reduces the fatigue life of the wind turbine. As a result, tower construction costs, operation and maintenance, necessary material and the overall cost of energy will increase in offshore scenarios [4].

In the past 40 years, energy dissipation and damping systems have been utilized as vibration control devices in buildings, bridges and other civil structures in an effort to reduce undesired motions due to wind and seismic loading [33]. Passive, semi-active and active structural control systems are currently being researched and utilized in the fields

of architecture and engineering to mitigate the effects of dynamic loads on such structures [15]. One new application for damping control devices that is being examined is their potential to decrease vibration in land based wind turbines and OWTs [2]. Wind turbines are constantly excited and stressed by wind loading and, in an OWT's case, wave loading. Wind turbines could benefit greatly from a structural control device that would reduce deflections and control vibrations.

This thesis examines different types of passive energy dissipation techniques used in civil structures for potential use in an OWT. The goal of this investigation is to optimize the dimensions of the TLCD so as to minimize the tower top displacement as well as the platform displacement for floating turbines. It should be noted that many passive types of damper systems have been modified with semi-active and active abilities that utilize feedback control and actuator technology [25]. Semi-active and active controls are not considered in this thesis. The possible passive systems have relative advantages and disadvantages, and the passive tuned liquid column damper (TLCD) has been selected for research and simulation when installed into the nacelle or platform of an OWT based on an analysis presented below. The results of the simulations show that the use of a TLCD can have positive results in reducing the overall tower top and platform motion in some offshore wind turbines, while in some cases it actually increases overall motion of the tower top and platform.

1.2 Overview of Thesis

As presented in this thesis, the implementation of a TLCD in OWTs is analyzed. Chapter 1 gives an introduction to the thesis as well as background and motivation. Chapter 2 presents a background of the current state of wind turbine technology including

offshore wind technology. Chapter 3 gives an overview of passive structural control devices that may be applicable for vibration reduction in an OWT. Chapter 4 analyzes design challenges and criteria for choosing a type of passive structural control system to be modeled in an OWT. From the examined devices, the TLCD is chosen based on its overall applicability. Chapter 5 presents a thorough examination of the TLCD and how its design and dimensions are specifically important in reducing a systems structural vibration. Chapter 6 begins the analysis of coupling the TLCD with an OWT model. The complexities of coupling TLCD dynamics with OWT systems are examined. Equations of motion are derived for limited DOF OWT coupled with TLCDs. Chapter 7 presents how the motion of the different TLCD-OWT systems are simulated using MATLAB. This includes developing and performing different simulation techniques and defining the input parameters for those methods. It also describes the program for an optimization routine that was built for finding optimum TLCD dimensions. Chapter 8 presents the optimization results. TLCD dimensions for an optimum non-uniform and uniform cross-sectional area TLCD and performance comparisons are made using the different simulation techniques. It also draws comparisons between optimized TLCD parameters and ideal tuned mass damper (TMD) values. Chapter 9 draws conclusions from the use of a TLCD in an OWT and comments on future research topics.

CHAPTER 2

BACKGROUND

2.1 Wind Turbine Technology

Over the past 40 years, onshore wind turbine development has increased due to the need for renewable energy production and technology advancement. In more recent years, wind turbines have been placed in offshore locations where the winds have lower turbulence and higher, more consistent speeds compared to most onshore locations. These locations provide a higher amount of possible energy extraction.

Suitable coastal and offshore areas are now being utilized to develop wind farms. This is advantageous, as a high density of the population in countries like the United States live near coastal regions. Placing wind turbines in offshore locations has the potential to reduce electricity transmission distances. Figure 2.1 shows the correlation between the highest wind classifications and population dense areas in the United States.

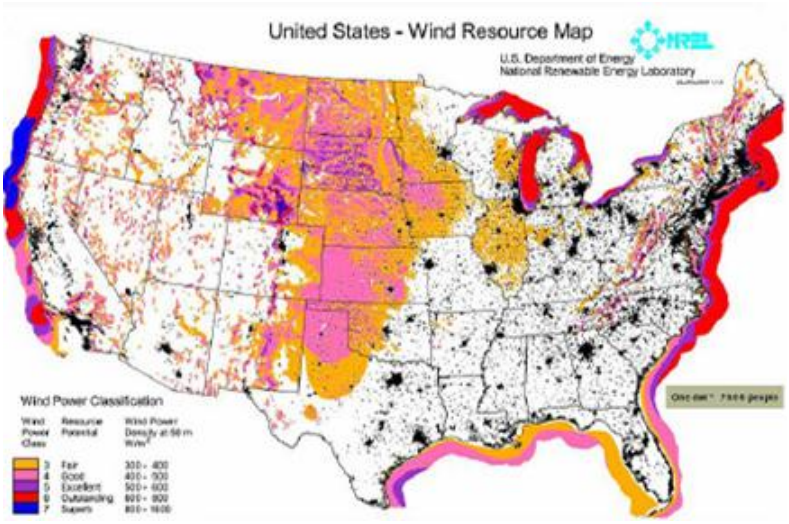

Figure 2.1: United States wind resource at 90 m height and population centers [21]

As technology has progressed over time, wind turbine size has also increased to capture more of the wind's energy. This is because the power captured by a wind turbine is proportional to the swept area of the rotor. The growth of wind turbines has generally led them to be placed in offshore locations due to the undesirable noise production and possible visual burden in an onshore area. Placing the turbines in offshore locations can diminish the possibly disturbing effects that they may have on the local population. A larger rotor size also experiences increased dynamic and stochastic loading. Less turbulence in offshore locations provides conditions that are more suitable for larger wind turbine rotors.

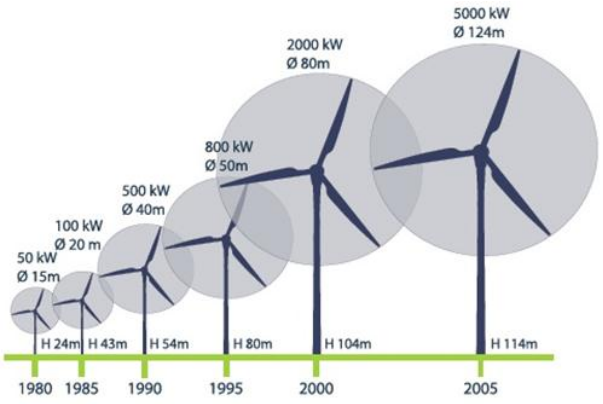

Figure 2.2: Year-to-year growth of wind turbine height and rotor diameter [12]

2.2 Offshore Wind Technology

There are currently different types of OWTs that have been developed for use in specific offshore locations based on geographical and climate characteristics as well as socio-economic need. OWTs can be classified based on location water depth. Fixed bottom foundations are placed in 0-60 m of water. Foundations of this type can be subclassified as shallow water foundations (0-30 m) and transitional depth foundations (30-60 m). Floating systems are typically used in depths deeper than 60 m [4].

2.2.1 Fixed Bottom Foundations

To date, fixed bottom foundation-based wind turbines have experienced growth and development in offshore locations in Europe and China. These types of wind turbines are limited to moderate water depths (0-60m) due to cost and physical constraints for driving foundations and the towers inherent flexibility.

2.2.1.1 Shallow Water Foundations

Shallow water foundations are typically used within a range of 0-30 m water depth. Figure 2.3 shows three different options for fixed bottom, shallow water OWT foundations. These include the monopile, the gravity base and the suction bucket. The monopile is put into the ground by pile-driving a foundational tube into the sea bed and mounting the turbine components via a transitional piece. The gravity base uses a large mass as the turbines ground attachment point. This mass keeps the tower fixed to the seafloor. The suction bucket is a wide hollow tube that is attached to the sea floor. Water is then removed completely from inside the tube. This creates a vacuum-like container that drives the bucket into the seabed and holds the turbine to the ocean floor. The use of each type of fixed-bottom wind turbine is highly dependent on ocean floor conditions. In this research, the monopile will be considered as a physical representation of all fixed bottom OWTs.

Figure 2.3: Current options for shallow water foundation wind turbines [4]

2.2.1.2 Transitional Foundations

As water depth increases, support systems for an OWT may need to include a wider base and multiple attachment points to the ocean floor to provide ample support. These transitional depth foundations are applicable in ocean depths of 30-60 m where simple fixed-bottom shallow water foundations are no longer applicable. Though no transitional foundations are analyzed in this research, they are presented to show other possible offshore foundation options. These include the tripod tower, guyed monopile, full-height jacket, submerged jacket with transition tube to tower and the enhanced suction bucket.

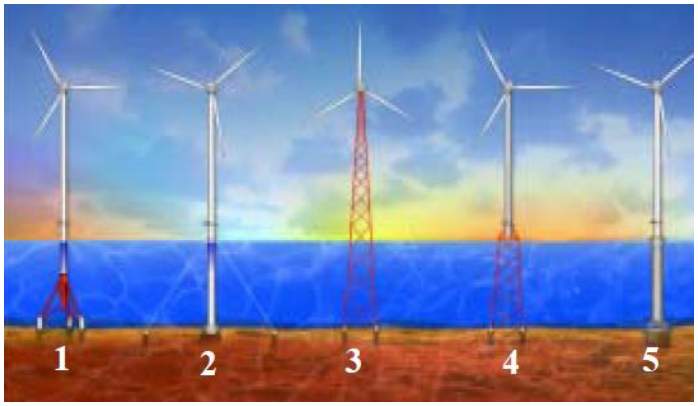

Figure 2.4: Transitional depth foundation technology [4]

2.2.2 Floating Systems

Water depth imposes many constraints on the use of fixed bottom OWTs. As the water depth increases beyond 60 m, difficulties due to cost and foundation installation for fixed bottom OWTs increase substantially. In these deep water locations, different types of floating technologies may then be used. These locations typically contain the highest and most consistent wind speeds, and floating technology provides accessibility for capturing these winds. Floating wind turbines are also more independent of seafloor conditions and can therefore be placed in a multitude of locations. It should be noted that all floating system technology is currently prototypical and not available commercially, but is being studied for potential offshore application.

There are three different types of floating systems that have been widely studied. These include the spar buoy, barge and tension leg platform (TLP). These types of floating systems utilize three different distinct methods for achieving stability.

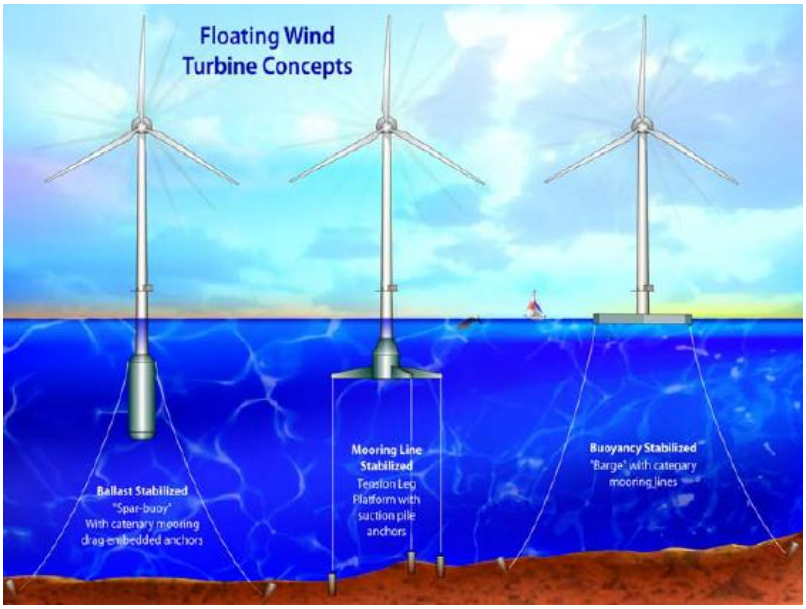

Figure 2.5: Concepts for floating wind turbines [4]

2.2.2.1 Spar Buoy

The spar buoy uses a ballast weight as its main method for achieving stability. This large weight is hung far below the center of gravity of the system inside of the spar. As the rotor is subjected to force, the ballast weight provides a righting moment to offset the motion induced by the rotor. This has the ability to offset pitch, roll and possibly heave motion. The spar buoy is held in place by catenary mooring lines and uses a large buoyancy tank to keep it afloat. The nature of the design of the spar makes it very susceptible to yaw induced motion.

2.2.2.2 Barge

The barge utilizes a distributed buoyancy system and a high water plane area to achieve stability. It uses this weighted water plane area for motion resistance and increased stability. Like the spar, it is also held in place by catenary mooring lines. The barges large water plane area does make it more sensitive to wave motion.

2.2.2.3 Tension Leg Platform

The TLP achieves stability through the use of mooring line tension. The TLP also contains a central spar which holds a buoyancy system and ballast weight to help offset any motion of the turbine. The TLP is not analyzed in this report, but is included for reference as a common floating wind turbine concept design.

2.3 Limited Degree-of-Freedom Systems

Stewart has developed equations of motion describing limited degree-of-freedom (DOF) models for the fixed bottom monopile, spar buoy, barge and TLP OWT systems

[24]. These limited DOF models are meant to capture the important dynamics of the respective systems, while still using relatively simple sets of equations. The equations are utilized to study the motion of each system. Parameter values of the baseline OWT systems that are used in this thesis include mass, inertia, stiffness, damping and turbine dimensions. These are found or derived from FAST input files. FAST is an aero-elastic simulator developed by NREL used to measure, predict and simulate the motion and response of horizontal axis wind turbines (HAWTs). It contains a number of input files that define specific wind turbine parameters used to describe different HAWT models. Parameters applicable to this thesis are described in Chapter 6.1 [6].

CHAPTER 3

STRUCTURAL CONTROL

3.1 Necessity for Structural Control Devices

Though wind energy has progressed greatly over the past 40 years, there are still many obstacles to overcome, especially in the offshore industry. Overall cost of energy is a huge factor in the placement and construction of OWTs. One area that can be improved upon is the structural vibration control of the turbine, tower and support components. Due to their large size and complexity, it is necessary to reduce the costs of OWTs by making them both more efficient and increasing overall fatigue life. One method for reducing unwanted vibration due to loading is to apply a structural control device. Structural control has been used extensively in civil structures such as buildings and bridges to offset seismic and wind induced vibrations. This involves installing a mechanism in a civil structure that will effectively reduce force-imposed excitation and increase the overall fatigue life of the system. OWTs offer an interesting opportunity for utilizing a structural control device. High dynamic forces can occur in OWTs due to wind, wave, and possibly ice loading. As wind turbine size continues to grow, the loading placed on a turbine will also increase. OWTs have the potential to benefit structurally from the use of vibration-damping mechanisms such as those presented in the following sections.

3.2 Overview of Structural Control

Structural control systems are used to mitigate unwanted vibrations that are induced on the main system. They can be designed in a number of forms. Active and semi-active systems utilize feedback control to improve the vibration reduction of a

structure. Passive systems are typically tuned to a certain frequency of a particular structure for vibration mitigation. This thesis will only examine passive structural control devices as the method for reducing vibrations in OWTs.

3.3 Passive Structural Control

In its simplest form, a structural control device uses no external energy to reduce vibration imposed on the main system. These are known as passive structural control devices. A key benefit to passive control is that once installed in a structure, they do not require any start-up or operation energy unlike active and semi-active systems. Passive control devices are active at all times until maintenance, replacement or dismantling is required. There are many different types of passive control systems examined in this project. Some structural control systems do not contain a spring-like component and are not tuned to any particular natural frequency. Types of this nature include the friction damper, the metallic yield damper and the viscous fluid damper. Other types of passive control systems contain a spring (or spring-like component) which is tuned to a particular natural frequency of the structure for maximum damping. These are known as tuned mass dampers (TMD). This thesis considers different types of TMDs including the pendulum damper and the tuned liquid column damper (TLCD).

3.3.1 Spring-less Damper Systems

3.3.1.1 Friction Dampers

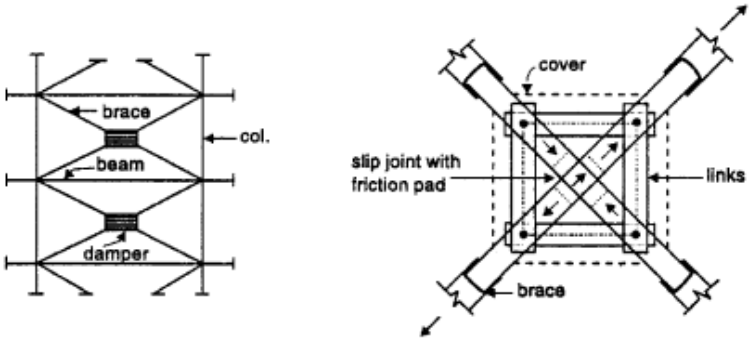

Figure 3.1: X-braced friction damper [22]

Friction dampers are a type of spring-less damper system [22]. They consist of two solid bodies that are compressed together. As a structure is subjected to a vibration, the two bodies slide against each other, developing friction that dissipates the energy of the motion. These devices have been built into structures and have been successful at providing enhanced seismic protection by being designed to yield during extreme seismic vibration. Wind loads do not provide enough shear force to activate these types of dampers. Though they are reliable at reducing seismic loading, they are not designed to slip during wind loading and they would not prove effective in a floating wind turbine. They are therefore discounted from the decision process.

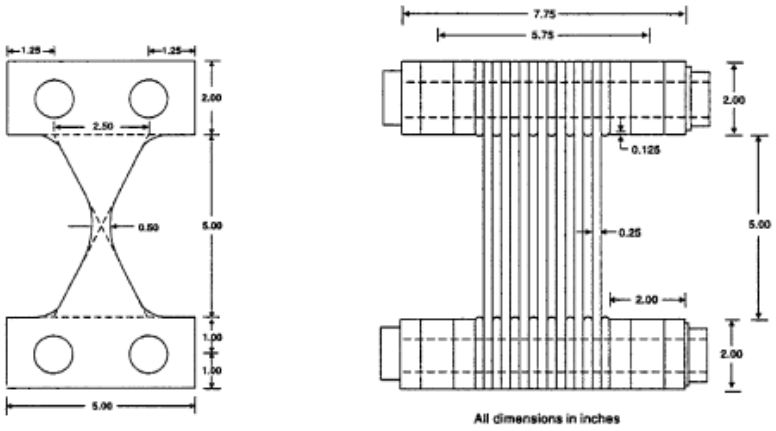

Figure 3.2: Metallic yield damper [1]

3.3.1.2 Metallic Yield Dampers

The second type considered for utilization is the metallic yield damper [1]. A typical design for this damper is a triangular or X-shaped plate that absorbs vibration through the inelastic deformation of the metallic material. These devices are known to have a stable hysteric behavior and long term reliability [27]. These types of dampers are usually installed in newly built and retrofitted buildings, and have been shown to be successful in reducing seismic loads.

3.3.1.3 Viscous Fluid Dampers

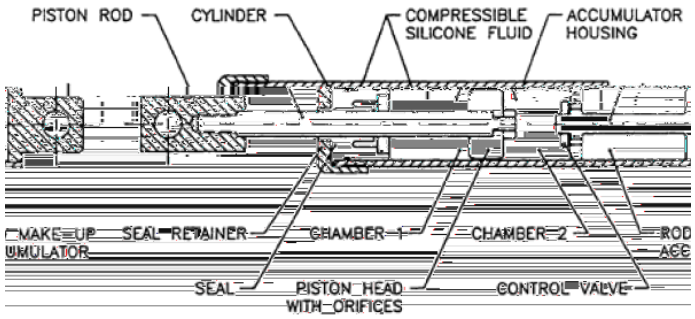

Figure 3.3: Viscous fluid damper [13]

Viscous fluid dampers (VFD) are another type of spring-less damper system [13]. Similar to shock absorbers, they consist of a closed cylinder piston that is filled with fluid, usually a type of silicon oil. The piston head contains orifices so that the fluid can move between the two chambers of the piston [7]. When excited, the movement through the holes generates friction, and subsequently heat, which dissipates the moving energy of the structure to which the VFD is attached. VFDs are typically installed or retrofitted as the diagonal in a building's brace frame. To provide optimal damping, buildings are often equipped with multiple VFDs in place of diagonal beams on many floors.

3.3.2 Tuned Mass Dampers

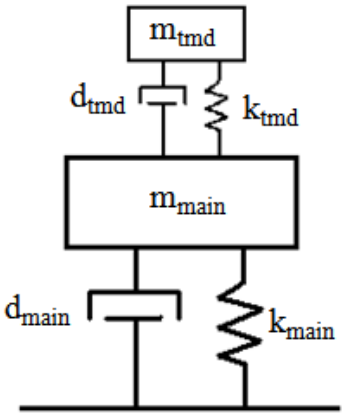

Figure 3.4: Simple tuned mass damper and structure system

TMDs are one classification of specific types of passive energy dampers. A TMD consists of not only a mass and damper, but also a spring that is tuned to one of the various frequencies of a structure. TMDs are typically tuned to the first resonant frequency of a structure to provide maximum damping. One trait that is more common in TMDs as opposed to other types of damper systems is that TMDs have been installed in tall buildings and towers for control primarily against wind-induced external loads [8]. As compared to some of the previously mentioned types of structural control, TMDs do

not have to overcome high slip loads resulting from extreme seismic forces to operate and will react to any amount of excitation. Because of this, they are more appropriate for reducing less extreme excitations such as those produced by wind and waves. There are many different types of passive TMD systems currently utilized and available for examination.

3.3.2.1 Pendulum Dampers

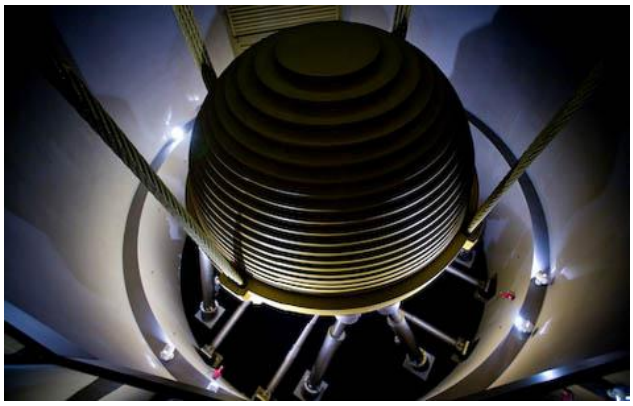

Figure 3.5: Pendulum TMD utilized for structural control in Taipei 101 [31]

One type of passive TMD that has been utilized in many tall buildings is a pendulum damper system. This system contains a large mass that is typically hung in an oil bath or left to swing freely with the motion of the structure. The mass swings in opposition to the structure's movement to provide damping. TMDs of this nature are used to mitigate wind-induced excitations, but have also shown the capability for reducing earthquake-type excitations [27].

3.3.2.2 Tuned Liquid Column Dampers

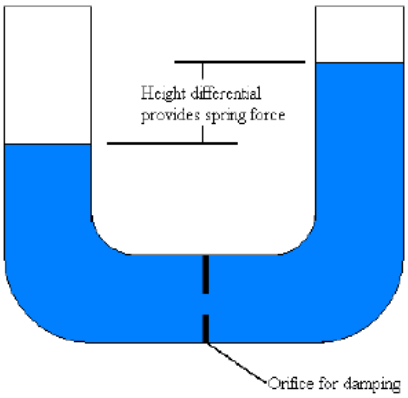

Figure 3.6: TLCD schematic [24]

Sloshing dampers that use liquid rather than a solid as their main mass have been utilized in civil structures. A modified form of the sloshing damper is the tuned liquid column damper (TLCD). A TLCD can be described as a U-shaped tube that is partially filled with a volume of liquid that acts as the mass of the damper. As the structure with an attached TLCD is excited, the liquid oscillates through the column and eventually helps to restore the system to equilibrium. The TLCD column usually contains one or more orifices that are sized to generate proper viscous damping [17]. The orifice generates a head loss in the column which is important for energy dissipation. Changing the dimensions of the TLCD has a large impact on the effectiveness. It has been experimentally shown by Basu et al. that wind turbines equipped with specific TLCDs may achieve reduced peak responses up to 55% under wind and wave loading in certain conditions. Implementations of TLCDs in experimental wind turbines have also shown an increase in fatigue life of the wind tower assembly [2].

CHAPTER 4

DESIGN CRITERIA AND CHALLENGES

4.1 Examining Design Challenges

Each type of control device has its own benefits and drawbacks. Many design challenges are considered when assessing the pros and cons of each system in order to obtain an optimal system for OWTs that will generate the lowest cost of energy. The following section will outline some potential concerns for choosing a damper system for an OWT. A final decision is then made regarding a specific damping device.

4.1.1 System Costs

One of the most important considerations in this thesis is deciding upon a vibration reduction system that will minimize fatigue loading while reducing overall cost. Costs that need to be considered for placing a structural control system in a floating wind turbine can include capital costs, installation, maintenance, and decommissioning. Maintenance on the turbines can become extremely costly due to the accessibility, restrictions imposed by weather, and the necessity for specialized service vessels [20].

Metallic yield dampers have been shown to effectively reduce the effects of extreme seismic loads. One disadvantage of this system is that when it is subjected to a large enough seismic load, the damper requires replacement [28]. Though a wind turbine may not be subjected to a seismic load of this size often, metallic yield dampers have not been shown to be effective at reducing smaller excitations such as those due to wind loading. These types of dampers are more suitable for onshore locations that are

subjected to extreme seismic disruptions where they are more accessible. Because of these reasons, the necessary replacement of the damper would be costly and taxing.

Pendulum dampers typically require a large mass relative to that of the system to offset motions. The mass is usually constructed of steel or another dense material. Using this amount of material requires a large amount of capital, which also includes lifting, installing and decommissioning a large mass of this nature.

Many sources have noted the low capital and maintenance costs of TLCDs compared to other types of damper systems [34]. One difference compared to pendulum dampers is that TLCDs utilize water as their mass, which can be pumped into or out of the column with ease and is also less expensive than a solid mass. When examining the use of a TMD in an offshore scenario, it could be logical to use a system that utilizes liquid as its mass. Thus, TLCDs are considered to be the most economical option.

4.1.2 Weight/ Size

Weight and size properties need to be examined when considering different types of damper systems. Wind turbine nacelles (as well as platforms and spars) are limited in the amount of free space that is able to house a damper system. Because the nacelle is also located high above the ground, installing a heavy damper system adds complexity to the installation and maintenance processes. Floating platforms such as the barge may be able to hold different types of damping systems because of their large size.

In considering the use of the viscous fluid damper (VFD), one would have to consider the structure of the wind turbine tower and nacelle. Most VFDs placed in buildings are attached as diagonal structural support braces. They are usually placed on each floor of the building, requiring a large number of dampers [7]. Because of their

design, it would be impractical to house these dampers in the nacelle because most motion occurs in the tower or platform. Also, wind turbine towers do not have the space or the infrastructure to accommodate a damper network system of this type.

Major restrictions with the pendulum damper are not only the large space that is necessary to house the damper, but also the dampers overall mass. Conventional pendulum dampers of this nature usually weigh approximately 4% of the total structure. Though current wind turbines do utilize pendulum dampers, exploring the use of lighter-weight TLCDs presents a viable alternative [16]. Research has shown that TLCDs can provide similar damping as compared to a pendulum damper while only weighing 2% of the wind turbines total effective mass [14]. This is possible because the displacement of the water through the orifice in the TLCD is able to provide similar damping to that of a pendulum type [2]. Provided that the necessary horizontal length is available, TLCDs also prove more efficient than other damper types with respect to volume and area utilization. It has been noted that a larger ratio of the horizontal length to the total length of the TLCD increases the effectiveness of the TLCD [19]. Efficiency may have to be sacrificed if the necessary horizontal and vertical space is not available.

4.1.3 Maintenance and Replacement

There are many difficulties associated with accessing and maintaining a damper system in a wind turbine nacelle or platform. Accessibility and maintenance in a tall wind turbine or underwater location can prove difficult. A damper system needs to be chosen that will minimize the amount of required maintenance while not sacrificing efficiency. Some types of damper systems, including the metallic yield damper require replacement after every impacting seismic event [28]. Upkeep and replacement of this type of system

would result in large maintenance and cost requirements. TLCDs have been shown to be beneficial over different types of damping technologies in many scenarios because of their ease of handling and few maintenance requirements [17].

4.1.4 Performance

Many of the noted structural control devices are designed to react to extreme loading. Metallic yield and friction dampers are designed more for extreme events such as earthquakes. The nature of the wind and wave forces imposed on an OWT is not typically as extreme as an earthquake. TMDs are specifically designed for this type of vibration reduction. Specialized TLCDs are shown to be even more effective than TMDs in particular cases. One positive aspect of the TLCD is that unlike other types of TMDs, they can dissipate very low amplitude excitations and are consistent over a wide range of excitation levels [23]. This gives them the ability to damp vibrations other than that of the natural frequency to which they are tuned and are more applicable to an OWT.

4.2 Chosen Method: TLCD

OWT Design Challenge	Friction Damper	Metallic Yield Damper	Viscous Fluid Damper	Tuned Pendulum Damper	Tuned Liquid Column Damper
Tuned to natural frequency of the system				X	X
Effective in reducing wind loads			X	X	X
Effective in reducing wave loads			X	X	X
Effective in reducing seismic loads	X	X	X	X	X
Do not require replacement after use				X	X
Don't need to overcome high slip loads				X	X
Low initial costs	X	X			X
Low maintainability costs			X	X	X
Applicable to offshore scenario				X	X
Aided by use of water as mass					X
Ease of installation	X	X			X
Applicable for placement in nacelle/platform				X	X
Applicable for placement in tower	X	X			
Weight/Volume	X	X	X		X
Overall performance in OWT				X	X

Table 4.1: Table showing benefits of each considered damper system

By analyzing the considerations listed in Table 4.1, the TLCD is the most practical choice for further evaluation in an offshore wind turbine. The following chapter will examine the TLCDs properties in depth and will formulate a method for designing a TLCD with optimal dimensions and characteristics for placing in the nacelle or floating platform of an OWT.

CHAPTER 5

TUNED LIQUID COLUMN DAMPERS

5.1 Physical Overview

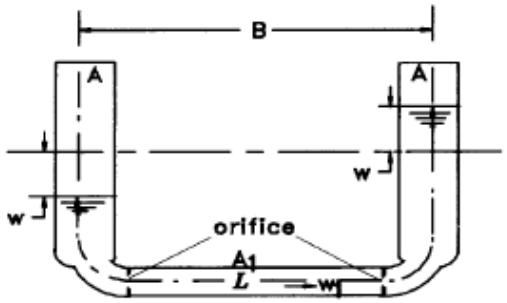

Figure 5.1: U-shaped TLCD with varying cross-sectional area [17]

A TLCD is designed to reduce the maximum amount of structural vibration of a civil structure due to wind, seismic and possibly wave loading. As previously outlined, a TLCD can be described as a U-shaped tube that is partially filled with a volume of liquid (usually water or a water/glycol mixture). The horizontal column of a TLCD usually contains one or more internal orifices used to generate energy dissipation [8]. These orifices can be sized according to the specific mode of the structure and the optimum achievable damping. The frequency of oscillation of the liquid in a TLCD is usually specifically tuned to the natural frequency of a structure to provide maximum damping [2]. As a structure vibrates, the liquid in the attached TLCD oscillates, opposing the motion of the structure. Vertical displacement of the water in the TLCD is then restored by gravity which provides the stiffness to the system [14]. From this offsetting motion, structural vibrations and bending moments are expected to be reduced and will result in an increase in the fatigue life of the structure [3]. The time to reach equilibrium in a

TLCD-structure system is expected to take shorter than an undamped system and the use of a TLCD also reduces the overall amplitude of the structure's motion.

5.2 TLCD Sizing Characteristics

The level of vibration reduction that a TLCD generates is completely dependent on its size and dimensional characteristics. There are many different variations of TLCDs that have been researched. There are a few major points that need to be considered.

- Setting the TLCD's mass to have an appropriate mass ratio is important when looking at a specific civil system, as the main system will determine the overall size and mass constraints of the TLCD.
- When designing a TLCD, it has been determined that increasing the cross-sectional area ratio ($\alpha = A/A_1$) of a TLCD can greatly shorten the length requirement compared to a TLCD with uniform cross-sectional area while suppressing the same level of structural vibration. This difference in column area size can be seen in Figure 5.1.
- A TLCD with a larger ratio of the liquid column horizontal length to its total length can reduce the maximum response of the structure more efficiently than that of a smaller ratio [10].
- Orifice size is also a critical parameter and impacts performance. The damping of a TLCD is highly dependent on orifice size and can affect how the TLCD performs overall. Watkins has shown that by using different orifice opening ratios, the frequency response of the TLCD can change [29-30].

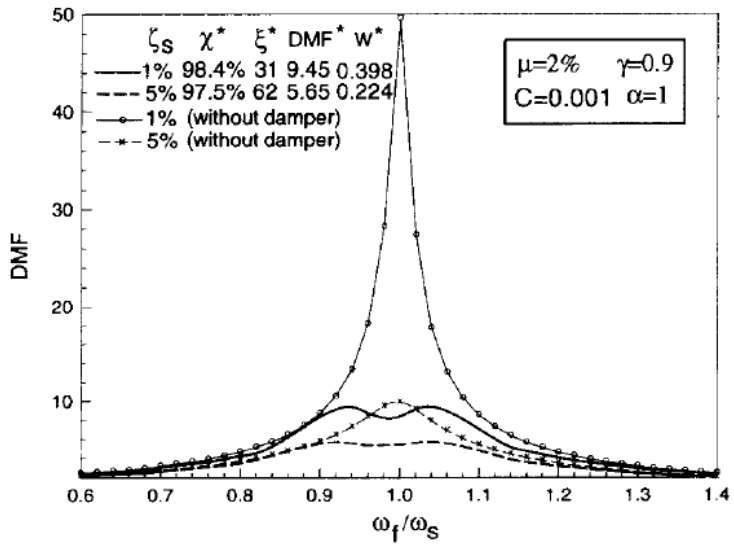

Figure 5.2: Examining the effects of structural damping on response of a structure with and without a TLCD [10]

All of the aforementioned characteristics are extremely important in designing an effective TLCD for an OWT. When chosen properly, optimal TLCD dimensions and damping levels can be obtained for reducing vibration when applied to an OWT.

5.3 TLCD Mathematical Modeling

TMDs have been studied extensively and equations of motion describing their behavior have been derived when utilized in a civil structure. Based off of these studies, Den Hartog's method for determining the vibration absorber parameters for an undamped system has proved successful in developing the equations of motion for a TLCD [9]. Using Den Hartog's methods, analytical formulas for determining the equations of motion for a uniform cross-sectional area TLCD have been derived by Sakai et al. [23]. Gao et al. have further developed the equations of motion for a U-shaped TLCD with varying horizontal and vertical cross-sectional areas [10]. This TLCD model is shown in Figure 5.1. It has been found that an increase in cross-sectional area ratio

(vertical/horizontal) can greatly reduce the length requirement when compared to a TLCD with uniform cross-sectional area in suppressing the same level of structural vibrations. This can also reduce the vertical liquid amplitude in the TLCD and could be an advantage when working within limited-size enclosures. Because of the size constraints within the nacelle and floating platforms of a wind turbine, the use of a TLCD that contains varying cross-sectional area is performed. A uniform TLCD analysis is also conducted to make performance comparisons.

The equations of motion for a TLCD with non-uniform cross-sectional area are derived by examining the potential and kinetic energy, continuity, as well as the forces from inertia and damping of a TLCD model. When examining a single-degree-of-freedom TLCD system on a horizontally translating main system, the equation of the liquid column motion is:

$$\rho A L_{ee} \ddot{w} + \frac{\rho A \zeta}{2} |\dot{w}| \dot{w} + 2\rho A g w = -\rho A_1 B \ddot{v}_s \tag{5.1}$$

Eqn. (5.1) involves the parameters of both the undamped main system and the dimensions and characteristics of the TLCD. In this equation, ρ is the liquid mass density, and g is the gravitational acceleration. A and A_1 are the cross-sectional areas of the liquid columns vertical and horizontal sections, respectively. $L_{ee} = L - B + \alpha B$ can be regarded as the length of an equivalent uniform liquid column with cross-sectional area A that possesses the same energy as the TLCD. L is the total length of the liquid column, B is the horizontal length of the TLCD and $\alpha = A/A_1$ is the area ratio. When $\alpha = 1$, the TLCD has a uniform cross-sectional area. w represents the liquid relative displacement in the vertical columns with over dots defining time derivatives; ζ is the coefficient of head loss

and v_s is the translational displacement or the main structure with over dots representing time derivatives.

For a one-degree-of-freedom, horizontally translating main system, the equation of motion (EOM) of the main structure with an attached TLCD can be written as:

$$m_s\ddot{v}_s + c_s\dot{v}_s + k_s v_s = P - \rho AB\ddot{w} - m_{TLCD}\ddot{v}_s \quad where \quad |w| \leq \frac{L-B}{2} \tag{5.2}$$

Where m_s, k_s, and c_s are the respective mass, stiffness and damping of the main structure. P is an external force. The defined constraint states that the absolute relative displacement of the water $|w|$ cannot exceed that of the vertical column height. This would cause water to flow over the top of the column, causing it to spill or nonlinearly hit a wall.

Because of the non-uniform column cross-sectional areas, the mass of the damper m_{TLCD} (which excludes the mass of the liquid container) can be expressed as:

$$m_{TLCD} = \rho A\left[\frac{B}{\alpha} - (L - B)\right] = \rho A L_{em} \tag{5.3}$$

L_{em} is the length of an equivalent uniform cross-sectional area liquid column with area A which has the same mass as the TLCD. Defining L_{ee} and L_{em} gives the ability to describe the characteristics of a TLCD with varying horizontal and vertical cross-sectional areas.

CHAPTER 6

TLCD COUPLING TO OFFSHORE WIND TURBINES

6.1 Baseline Wind Turbine

In order to approximate the properties of a wind turbine for use in the simulations, a baseline turbine model is used for analysis. The turbine chosen is the widely-studied NREL 5 MW wind turbine model. Table 6.1 outlines relevant turbine properties [6].

Rating	5 MW
Rotor Orientation	Upwind, 3 blades
Rotor and Hub Diameter	126 m, 3 m
Hub Height	90 m
Overhang, Shaft Tilt, Pre-cone	5 m, 5 m, 2.5°
Rotor Mass	110,000 kg
Nacelle Mass	240,000 kg
Tower Mass	347,460 kg
Coordinate Location of Overall COM	(-0.2 m, 0.0 m, 64.0 m)
Nacelle Dimensions	18 m x 6 m x 6 m

Table 6.1: Table showing physical properties describing the NREL 5 MW baseline turbine model

6.2 Turbine Limited DOF Model Development

Stewart has developed limited DOF equations of motion for the monopile as well as the three previously noted floating OWTs [24]. Stewart's research involved the use of an idealized TMD when placed in varying locations of a specific turbine to reduce displacements and fatigue. In this chapter, Stewart's equations describing the motion of the monopile, barge and spar buoy with an attached TMD are modified to include the use of a TLCD. The TLCD-wind turbine structure equations can be derived and used to model the motion of a wind turbine with attached TLCD in a simplistic, yet realistic and time-efficient manner. In order to develop equations of motion for each limited DOF

system, equations developed by Gao et al. describing a non-uniform TLCD need to be considered [10]. The issue when using the equations for the TLCD written by Gao et al. is that they are written to describe the TLCD and main structure in translational motion. To make them more physically accurate to the model, modifications need to be made to these equations so that they experience rotational motion. It should be noted that the developed equations of motion for the TLCD are written in a reference frame that is relative to the motion of the tower. Small angle approximations are also made because motions never exceed a few degrees. It is also assumed that all motion will be in the fore-aft direction in accordance with the orientation of the TLCD.

6.3 Monopile

Stewart's equations for the two degrees of freedom of concern (the rotational tower bending DOF and the translational TMD DOF) are used for analyzing the motion of the monopile. The developed model similarly contains two degrees of freedom: a tower bending DOF and a TLCD DOF. The tower is modeled as an inverted pendulum with rotary damping and stiffness in the tower base. Due to the nature of the monopile, it is only logical to place the damper system in the nacelle. The limited DOF model for the monopile coupled with a TLCD in the nacelle is shown in Figure 6.1. The *t* subscript and the *TLCD* subscript represent the tower and tuned mass damper DOF, respectively. *m*, *k* and *d* are the mass, stiffness and damping of each system, respectively. It is noted that the mass of the rotor-nacelle assembly (RNA) is included in the tower mass. θ represents the rotation of the system in degrees while the over dots represent time derivatives. w_{TLCD} is the displacement of the water inside the TLCD. *g* is the acceleration due to gravity. R_y is the ground reaction force.

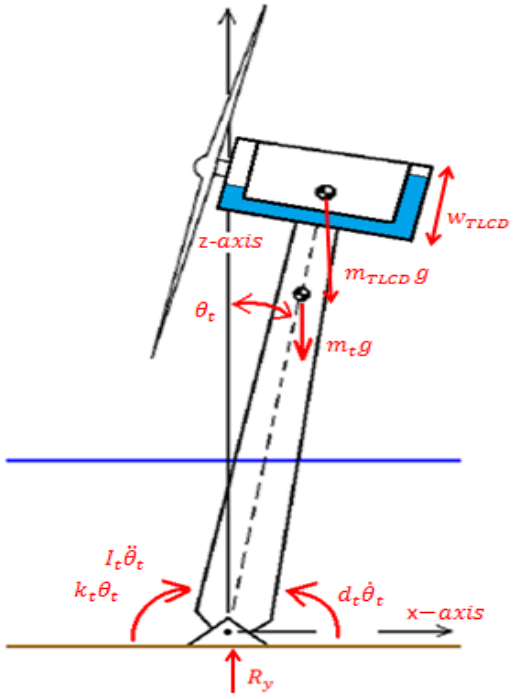

Figure 6.1: Diagram of the limited DOF monopile-TLCD model

6.3.1 Monopile-TLCD Equations of Motion

Equations for the two degrees of freedom of concern are now derived. These equations are written to describe the fore-aft motion of a TLCD when attached to the nacelle of a monopile wind turbine. Eqn. (6.1), describing the acceleration of the water inside of the TLCD is found by redefining Eqn. (5.1) in a rotational reference frame. To relate this to the rotational equations derived by Stewart, a gravity force proportional to θ_t must be included in the equation as well as a term that describes the inertia of the water movement inside the horizontal section of the TLCD. The EOM for the TLCD DOF can be written as followed:

$$\rho A L_{ee}\ddot{w} = -2g\rho A w - \frac{\rho A\zeta}{2}|\dot{w}|\dot{w} - \rho A_1 B R_{TLCD}\ddot{\theta}_t + \rho B A_1 g\theta_t \qquad (6.1)$$

In Eqn. (6.1), each term describes a specific force contribution to the TLCD. The first term on the right-hand-side represents the "stiffness" of the TLCD and the second

term represents the non-linear damping force due to the viscous flow in the column. These two terms are taken verbatim from Gao et al. The third term represents the inertial force on the TLCD due to the accelerating reference frame of the tower. Because this term was first described in a translational reference frame, the original term to describe the acceleration of the structure was replaced with $R_{TLCD}\ddot{\theta}_t$. The fourth term is added to describe the gravity force of the TLCD as a function of θ_t.

Eqn. (6.2) describing the tower DOF with a TLCD is generated by substituting Eqn. (6.1) into Stewart's equation for the tower bending DOF and simplifying. Since water is moving inside of the TLCD, there is a moment at the base of the tower that needs to be considered. Terms that describe gravitational moments due to the TLCD as well as the displaced water inside the TLCD also needed to be included. The tower DOF EOM can then be written as followed:

$$\left(I_t - \frac{\rho B^2 {R_{TLCD}}^2 A_1}{L_{ee}} + m_{TLCD}{R_{TLCD}}^2\right)\ddot{\theta}_t = m_t g R_t \theta_t - k_t\theta_t - d_t\dot{\theta}_t + \frac{2\rho ABR_{TLCD}g}{L_{ee}}w + \frac{\rho ABR_{TLCD}\zeta}{2L_{ee}}|\dot{w}|\dot{w} - \frac{\rho AB^2 R_{TLCD}g}{\alpha L_{ee}}\theta_t + \rho AgBw \tag{6.2}$$

On the left side, I_t is the tower inertia. The second term describes a moment on the tower due to the acceleration of the horizontal mass of the TLCD in the tower reference frame. The third describes the inertia due to the mass of the TLCD and its distance from the base. On the right side of the equation the terms include the gravity moment on the tower, tower stiffness, tower damping, and the equivalent TLCD spring moment proportional to water displacement, TLCD damping moment proportional to TLCD velocity, gravity moment due to the rotation of the tower, and the gravity moment from the displaced water in the TLCD.

6.4 Barge

Because the barge floats, it must be written with an additional DOF for the floating platform. The TLCD can potentially be placed in either the tower or the platform in order to examine the motion reduction capabilities. This results in two sets of equations of motion. The limited DOF model for the barge coupled with a TLCD in the nacelle and in the platform is shown in Figure 6.2. The *p* subscripts represent the added platform DOF.

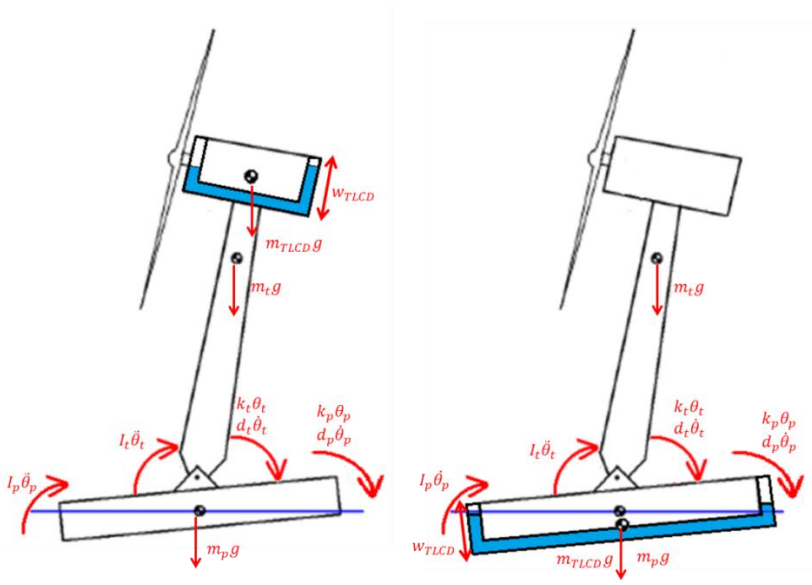

Figure 6.2: Diagram of the limited DOF barge-TLCD model with TLCD in nacelle (left) and platform (right)

6.4.1 Barge-TLCD Equations of Motion

6.4.1.1 TLCD in Barge Nacelle

Equations can be written for the barge model with a TLCD in the nacelle. In this model, three DOFs are of concern: the tower, the platform and the TLCD. Placing a TLCD in the nacelle of the turbine would be similar to that of the monopile, but with additional motion from the platform. An analysis was done similar to that of the

monopile for developing the equations of motion. The EOM for the TLCD DOF can be written as followed:

$$\rho A L_{ee}\ddot{w} = -2g\rho Aw - \frac{\rho A\zeta}{2}|\dot{w}|\dot{w} - \rho A_1 B R_{TLCD}\left(\ddot{\theta}_t + \ddot{\theta}_p\right) + \rho B A_1 g\left(\theta_t + \theta_p\right) \quad (6.3)$$

The addition of a floating platform can add some complexities to the model, but these can be taken into account rather simply. It is easy to see that Eqn. (6.3) is extremely similar to Eqn. (6.1), except that the water motion inside of the TLCD is also dependent on the platform motion.

The motion of the tower is also dependent on the platform motion. This leads to the gravity force from the leaning tower and the displaced TLCD being dependent on both the platform and tower displacement. Also, the platform acceleration provides an inertial force on the tower, as shown in the first term on the right hand side. The tower DOF EOM can then be written as followed:

$$\left(I_t - \frac{\rho B^2 {R_{TLCD}}^2 A_1}{L_{ee}} + m_{TLCD}{R_{TLCD}}^2\right)\ddot{\theta}_t = -I_t\ddot{\theta}_p + m_t g R_t\left(\theta_t + \theta_p\right) - k_t\theta_t - d_t\dot{\theta}_t + \frac{2\rho ABR_{TLCD}g}{L_{ee}}w + \frac{\rho ABR_{TLCD}\zeta}{2L_{ee}}|\dot{w}|\dot{w} - \frac{\rho AB^2 R_{TLCD}g}{\alpha L_{ee}}\left(\theta_t + \theta_p\right) + \rho AgBw \quad (6.4)$$

The platform DOF EOM is written as:

$$I_p\ddot{\theta}_p = -d_p\dot{\theta}_p - k_p\theta_p - m_p g R_p\theta_p + k_t\theta_t + d_t\dot{\theta}_t \quad (6.5)$$

The model approximates various forms of damping (i.e. hydrodynamic and wave damping) and groups them into the barge damping constant, d_p. Restoring moments from the movement of the center of buoyancy and angular displacement as well as mooring lines are also grouped into the barge stiffness term, k_p. Stiffness is also provided in platform pitching motion by the ballast term: $m_p g R_p \theta_p$.

6.4.1.2 TLCD in Barge Platform

Due to the large available area of the barge, it is conceivable to attach the TLCD to the platform. This gives the opportunity for the TLCD to have an overall larger size and mass with expanded length dimensions, potentially increasing the TLCDs effectiveness. The application of a TLCD with a larger L_{ee} has the potential to more effectively damp out lower platform frequencies. The equations are generated by moving the TLCD related terms in Eqns. (6.3)-(6.5) from the tower DOF to the platform DOF. The EOMs for the TLCD, tower and platform DOFs are written below. The equations are extremely similar to when the TLCD is in the nacelle except that the platform DOF now contains the TLCD terms.

$$\rho A L_{ee}\ddot{w} = -2g\rho Aw - \frac{\rho A\zeta}{2}|\dot{w}|\dot{w} - \rho A_1 B R_{TLCD}\ddot{\theta}_p + \rho B A_1 g\theta_p \tag{6.6}$$

$$I_t\ddot{\theta}_t = -d_t\dot{\theta}_t - k_t\theta_t - I_t\ddot{\theta}_p - m_t g R_t\left(\theta_t + \theta_p\right) \tag{6.7}$$

$$\left(I_p - \frac{\rho B^2 {R_{TLCD}}^2 A_1}{L_{ee}} + m_{TLCD}{R_{TLCD}}^2\right)\ddot{\theta_p} = -d_p\dot{\theta}_p - k_p\theta_p - m_p g R_p\theta_p + k_t\theta_t + d_t\dot{\theta}_t +$$

$$\frac{2\rho ABR_{TLCD}g}{L_{ee}}w + \frac{\rho ABR_{TLCD}\zeta}{2L_{ee}}|\dot{w}|\dot{w} - \frac{\rho AB^2 R_{TLCD}g}{\alpha L_{ee}}\theta_p + \rho AgBw \tag{6.8}$$

6.5 Spar Buoy

Similarly to the barge, it is possible to put a TLCD in the nacelle of the spar or in the spar itself. The spar has a large vertical length, which can potentially accommodate an effective TLCD. Two models are therefore developed to represent the placement of the TLCD in the nacelle and the spar. There is very little difference in the development of the spar buoy model when compared to the barge model. The limited DOF model for the spar buoy coupled with a TLCD in the nacelle and in the spar is shown in Figure 6.3.

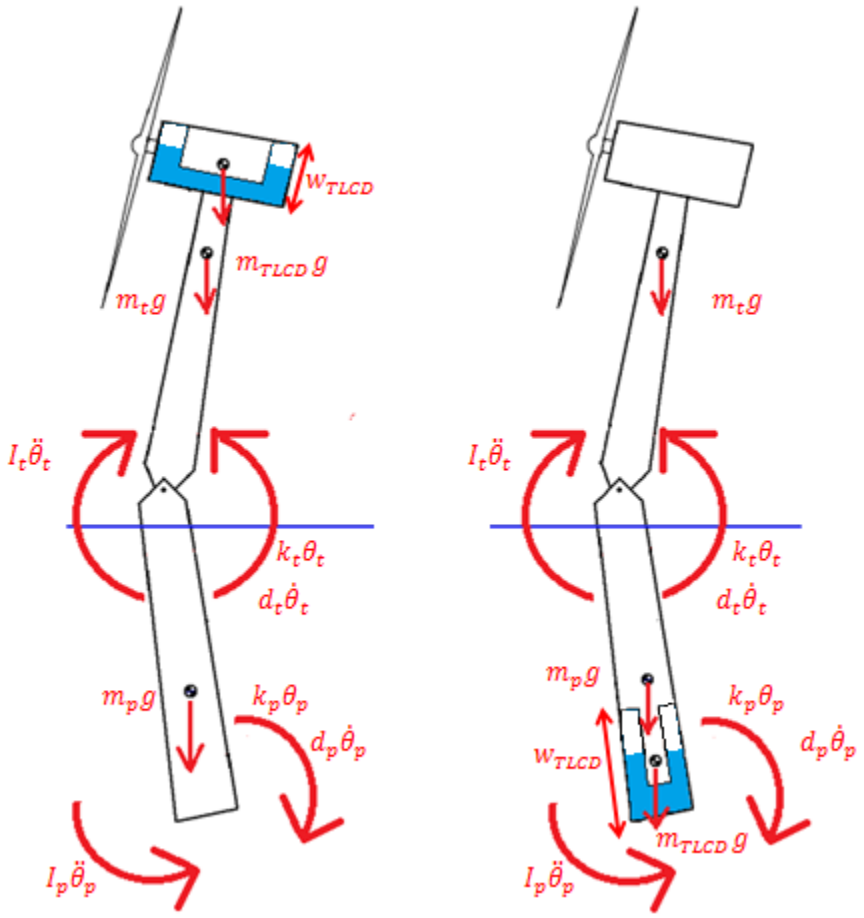

Figure 6.3: Diagram of the limited DOF spar buoy-TLCD model with TLCD in nacelle (left) and platform (right)

6.5.1 Spar Buoy-TLCD Equations of Motion

6.5.1.1 TLCD in Spar Buoy Nacelle

The equations of motion for the TLCD in the spar buoy nacelle are identical to that of the barge with the TLCD in its nacelle (Eqns. (6.3)-(6.5)). The only changes are the new definitions of the tower and platform property values, which are defined by the spar geometry and properties.

6.5.1.2 TLCD in Spar Buoy Platform

The equations of motion for the TLCD in the spar buoy nacelle are identical to that of the barge with the TLCD in its platform (Eqns. (6.6)-(6.8)). Once again, the only differences are the physical parameters describing the tower and the platform. The TLCD dimensions also need to be altered to fit within the constraints set by the spar.

CHAPTER 7

SIMULATING THE TURBINE-TLCD SYSTEMS

7.1 MATLAB Routine

In order to simulate the motion of the TLCD-monopile model in the time domain, MATLAB is utilized. An .m file is written that defines the TLCD, tower and platform variables for each system. The file allows the user to switch between turbine models and locations of the TLCD within those models. The .m file links to a number of function files that contain the EOMs of each of the DOFs of the systems. The built in MATLAB function ODE45 is utilized to integrate the equations of motion.

7.1.1 Initial Perturbation Method

A simple way to view the overall motion of the tower without giving it a specific forcing function is to perform an initial perturbation test on the system. This gives an overall impression of how the system reacts to a given initial displacement. To perform this, the system is given an initial displacement at time zero and allowed to oscillate freely for 100 seconds. Important system properties can be read from the initial perturbation test, including natural frequencies and damping properties of each DOF. A constant thrust force is also imposed on the tower top to simulate a constant wind force. This is a simple method for analyzing an imposed wind force. It is defined to be 500 kN. In the case of the monopile, the initial perturbation of the tower is 1.4 m. For each floating system, the platform pitch is given an initial displacement of 5 degrees from the vertical centerline of the system and is allowed to oscillate. To perform these simulations, defining the turbine parameters that aren't explicitly stated in FAST is necessary. This

includes turbine and platform stiffness and damping. When FAST was run using the applicable turbine parameters for the baseline 5 MW turbine, the natural frequency of each DOF can be extracted from the responses of each particular OWT. The stiffness values of the models are defined so that their natural frequencies match those of FAST. The damping values are chosen so that the limited DOF model responses fit closely with the FAST simulations.

7.1.2 External Forcing Method

A more realistic approach to analyze the motion of an offshore wind turbine system is to impose real time forcing that mimics aerodynamic and hydrodynamic loads. An aerodynamic thrust force and hydrodynamic pitching moment that are calculated in FAST are applied to the limited DOF models for each system. As the implementation of a TLCD to FAST-SC is not yet conceivable, this method is used to make the output of system as similar as possible to the outputs given in FAST from the simulation of an OWT in realistic conditions. The stiffness values used in this method are the same as the initial perturbation method. Due to the uncoupled nature of the forcing functions and the OWT system, the application of an aerodynamic and hydrodynamic forcing function required specific tuning of the damping values. The damping values were tuned from the original values used in the perturbation method because the addition of aerodynamic and hydrodynamic forces causes additional damping on the structural motion. The following section outlines the method for developing an applicable aerodynamic thrust force and hydrodynamic pitching moment.

7.1.2.1 Shinozuka Method

To perform the external forcing method, realistic aerodynamic thrust and hydrodynamic pitching moment time series files need to be defined. These are generated using FAST. The tower and platform DOFs are turned off in FAST so that the motion induced forces can be ignored. 1200 second simulations are carried out using turbulent wind and stochastic wave forcing. The characteristics of the wind and waves that are imposed using the external forcing method are defined in the FAST input files. The wind has a mean of 10 m/s, while the waves are defined by a JONSWAP spectrum with a significant wave height of 3.7 m and a peak spectral period of 14 s. The thrust force and pitching moments imposed on the tower and platform of each turbine model are extracted by examining the output files. Due to design differences in the limited DOF models and the FAST models, new forcing functions based off of the FAST thrust force and pitching moments need to be created. The so-called Shinozuka method (without jitter) is used to generate a time series of aerodynamic thrust and platform pitching moment data from the spectra of these signals from the FAST simulations [26]. This is implemented using an original code. The method works by taking a PSD of the original data time series and examines a range of frequencies of interest in the PSD. The PSD is divided into N intervals. At the interval midpoint frequency, sine waves are generated, each with a random phase angle and amplitude. A superposition of the waves is then produced and scaled by the amplitude of the spectra. The sum of the sine waves results in a new time series that contain the appropriate frequency content of the target spectra. Figure 7.1 shows an example of how the Shinozuka method generated synthesized data for the barge platform pitching moment based on simulated FAST data. These plots include the old and new time series as well as the frequency spectrum of each of the time series.

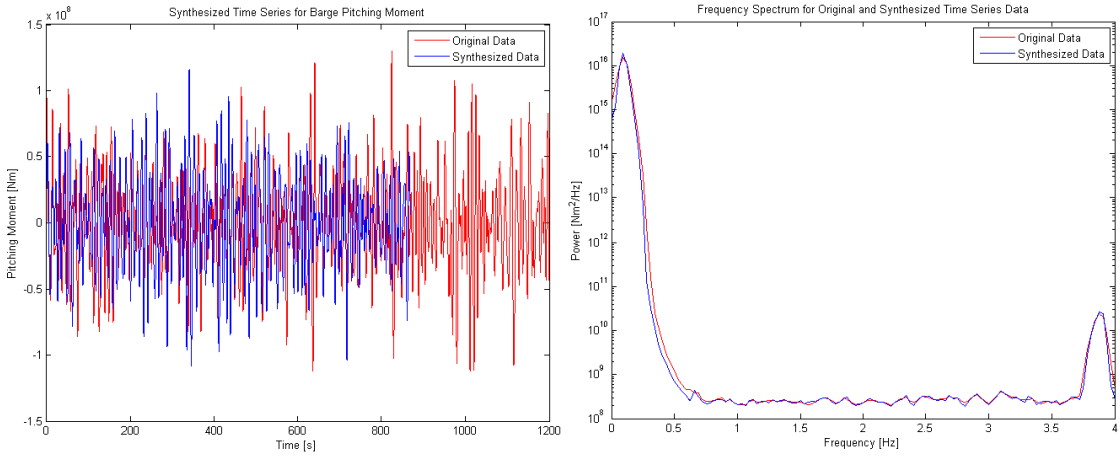

Figure 7.1: Example of original and synthesized pitching moment data

7.1.2.2 Aerodynamic Thrust and Damping

As previously mentioned, a single aerodynamic forcing time series was created and imposed on each system. This is based on the output of a FAST simulation of a monopile with the tower DOF turned off. However, many modifications needed to be made to the aerodynamic thrusting function. Wind forcing provides a large amount of aerodynamic damping to the system. The aerodynamic and tower damping are not coupled in the limited DOF models. To include the aerodynamic damping, it was recognized that the aerodynamic thrust and damping on a wind turbine can be determined using a first order Taylor series approximation. This can be presented as: $T(t) = T_0 + \frac{\delta T}{\delta t}\Delta t$. The thrust on a wind turbine rotor is defined as $T = \frac{1}{2} C_T \rho \pi R^2 U^2$ where C_T is the thrust coefficient, R is the rotor radius and U is the free stream wind speed. Substituting these terms into the Taylor series:

$$T(t) = T_0 + \rho \pi R^2 C_T \bar{U} \dot{U} \cdot \Delta t \tag{7.1}$$

In Eqn. (7.1), the first term, T_0 represents the thrust generated in the previous section using the Shinozuka method for each time step. The second term represents the aerodynamic damping. In this implementation, R = 63 m, ρ = 1.225 kg/m^3, C_T = 8/9 and

the mean wind speed, $\bar{U}$ =10 m/s. The instantaneous velocity $\dot{U}$ is found by multiplying the instantaneous change in tower pitch angle by the rotor height ($\dot{U} = \dot{\theta}_t R_{rot}$).

7.1.3 Baseline Simulations

Baseline results can be generated for the motion of OWTs without an attached TLCD when subjected to the initial perturbation and external forcing methods. These baseline results can be used as a quantitative comparison to evaluate the effectiveness of an added TLCD. The relevant outputs noted in this section are the standard deviation of the motions for each DOF. When simulating the monopile, the standard deviation of the tower top displacement (St.Dev.TTD) and the standard deviation of the water displacement (St.Dev.wDisp) are examined. When looking at the barge and the spar, which contain floating platform DOFs, the standard deviation of the platform pitch (St.Dev.PlatPitch) is also studied. In order to make sure that the motion of the water is held within constraints defined by the problem, the maximum water displacement (Max.wDisp) is also noted for each case.

7.2 TLCD Optimization

The goal of this investigation is to optimize the dimensions of the TLCD so as to minimize the St.Dev.TTD as well as the St.Dev.PlatPitch for floating turbines. This motion is used as a measure of fatigue loading on the structure. Reducing the TTD and PlatPitch reduces the overall fatigue of the system. All dimensions of the TLCD depend on the independent parameters: α, B, L, ζ. The independent variables need to be constrained to realistic values. These constraints are set by the nacelle and platform dimensions as well as the physical characteristics of the TLCD. The TLCD mass, m_{TLCD}

is pre-defined by the location of the TLCD according to the appropriate mass ratio values for the nacelle and platforms. Each dependent variable used to define the coupled TLCD-turbine EOMs can be determined from these independent parameters. These dependent variables include L_{ee}, L_{em}, the natural frequency of the TLCD, ω_{TLCD}, the height of the water column, H, and the vertical and horizontal column cross-sectional areas, A and A_1. Once each of the TLCD parameters are defined, simulations can then be performed. A summary of how the dependent variables are defined is presented in Table 7.1.

$\omega_{TLCD} = \sqrt{\frac{2g}{L_{ee}}}$	$L_{em} = \left[\frac{B}{\alpha} + (L - B)\right]$	$L_{ee} = L - B + \alpha B$
$H = \frac{L - B}{2}$	$A = \frac{m_{TLCD}}{\left[\rho * \left[\left(\frac{B}{\alpha}\right) + (L - B)\right]\right]}$	$A_1 = \frac{A}{\alpha}$

Table 7.1: Table showing definitions of dependent TLCD variables

7.2.1 Deterministic Sweep

A deterministic sweep is utilized in MATLAB as an optimization routine to find the optimum values of the TLCD variables. The optimization routine was written so that the program runs through the range of values set by the constraints for the independent parameters. These constraints are defined in the following sections. The routine changes the value of one parameter at a time so that every possible combination of values is analyzed. It then uses these values to run a single simulation of the coupled TLCD-turbine system in MATLAB. A matrix of outputs is generated. If the given parameters produce outputs that violate the constraints, the TLCD values are discarded. If the given parameters are within the constraints, the program outputs the TLCD dimensions as well

as the St.Dev.TTD, St.Dev.wDisp and St.Dev.PlatPitch (when applicable). Once all of the combinations of TLCD parameters are simulated, the program finds the set of TLCD parameters that produce the lowest St.Dev.TTD and outputs them. These are considered the optimal TLCD values for that case.

7.2.2 Nacelle Constraints

Figure 7.2: Wind turbine nacelle with exterior TLCD

The values generated by the deterministic sweep need to be bounded by the physical constraints of the problem. When the TLCD is placed inside (or possibly outside) of the nacelle, regardless of the type of OWT, the constraints can be determined based on the nacelle dimensions and the limits of the TLCD liquid motion. This set of constraints applies to all OWT models. Moreover, by applying certain constraints based on physical intuition, the overall parameter space can be greatly reduced thus limiting computation time. When placed in the nacelle, TLCD mass values range between 10,000 kg – 40,000 kg. Explanation of this is found in Chapter 8.1. To fit a TLCD within the nacelle, its dimensions are constrained by the following parameters:

1. It is noted by that having a TLCD with a large γ (γ=*B*/*L*) is more effective than a TLCD with a small γ (initial simulations confirmed this result) [3]. Given a nacelle length of 18 m, it is decided to keep *B* fixed at a maximum realistic value of 16 m.
2. The vertical water travel is constrained according to the formula $max|w| \leq \left[\frac{L-B}{2}\right] * 0.9$. This constraint states that the water displacement cannot go above or below the height of the vertical column of the TLCD, *H* (which is equal to the expression in the square brackets). A small safety factor of 0.9 is also employed. This specific constraint is applied after a simulation is performed to see if the given parameters are considered feasible.
3. It is desired to maximize the water displacement so as to reduce the tower top displacement as much as possible. To gain maximum water displacement, it is determined that the resting position of the water should be approximately half way between the height of the nacelle to maximize the range of vertical motion. The initial vertical column height constraint range is then defined to be between 2.5 and 3.5 m.
4. Given a nacelle height of 6 m, the total length, *L*, of the TLCD must be less than 28 m. Because of the need for ample space for water displacement discussed in #3, a more narrow constraint must be placed on *L*. Due to the limit set on the water motion given in the 3rd constraint; it is found that the TLCD length must be between 21-23 m.
5. The ratio of the vertical to horizontal column cross-sectional areas, α, must also be constrained. Given that it is possible to attach the TLCD to the outside of the nacelle, area ratio constraints can be somewhat relaxed. The TLCD will be constrained to having an $\alpha \leq 10$.

6. Gao et al. have performed a number of optimizations for U-shaped TLCDs and have determined an optimum ζ for each of their configurations. The constraint range for finding an optimum ζ in the following TLCD analysis is somewhat determined by the range obtained by Gao et al. The constraint is set to $0 < \zeta \leq 500$ [10].
7. It is also determined that the vertical column cross-sectional area should not be oversized. This is due to aesthetics and overall size constraints within or outside of the nacelle. Having a large exposed TLCD area outside of the nacelle may disrupt airflow. It is therefore decided to make the $A \leq 4$ m^2 and $A \geq 0.1$ m^2.

$B = 16$ m	Defined by nacelle dimensions
$max\|w\| \leq \left[\frac{L-B}{2}\right] * 0.9$	Maximum water displacement cannot exceed height of vertical TLCD column with safety factor
$\frac{L-B}{2} < 3.5, \frac{L-B}{2} > 2.5$	Set according to nacelle dimensions and vertical water displacement values
21 m $< L <$ 23 m	Set according to nacelle dimensions and vertical water displacement values
$0.1 \leq \alpha \leq 10$	Made within reason for size constraints
$0 < \zeta \leq 500$	Set wide range of ζ
0.1 m$^2 \leq A \leq 4$ m^2	Set reasonable range for A

Table 7.2: Table showing summary of nacelle TLCD dimensional constraints

7.2.3 Barge Platform Constraints

The dimensions of the barge impose new constraints for the TLCD. The barge has a 40 m x 40 m x 10 m platform. Therefore, the constraints can be determined based on the barge dimensions and the limits of the TLCD liquid motion. It is decided to limit the size of the TLCD so that the largest conceivable TLCD will be able to "wrap around" the bottom and sides of the barge. Any designs smaller than this would have to be built into the platform. This could increase the barge's construction complexity. Placing the TLCD in the platform allows the barge to hold a much higher TLCD mass value. These mass

values range between 100,000 kg - 400,000 kg. Explanation for this decision is found in Chapter 8.1. To fit a TLCD to the bottom of the barge, its dimensions are constrained by the following considerations:

1. The TLCD will be attached to the bottom of the platform. This constrains the TLCD horizontal length, *B* to be within a certain value. It is determined that if the TLCD were to wrap around the barge, *B* must be longer than the platform length. It is decided to let *B* range between 1 m < *B* < 45 m so that the optimization can explore all possible configurations.
2. Similarly to the nacelle, it is necessary to constrain the vertical water displacement in the TLCD. The vertical water travel must be constrained according to the formula $max|w| \leq \left[\frac{L-B}{2}\right] * 0.9$.
3. It is desired to maximize the water displacement so as to reduce the tower top displacement as much as possible. To gain maximum water displacement, it is determined that the resting position of the water should be approximately half way between the height of the barge to maximize the range of vertical motion. The initial vertical column height constraint range is then defined to be between 0.5 and 5.5 m.
4. Given a platform height of 10 m with some additional space, as the TLCD could possibly be placed on the outside of the barge, *L* must be less than about 60 m. Because of the need for ample space for water displacement, a more narrow constraint must be placed on *L*. Due to the limit set on the water motion given in the 2nd constraint; it is found that the TLCD length must be less than 56 m. L is also constrained so that it can't be less than 1 m.

5. Because the barge is going to have a low natural frequency, the value of L_{ee}, which defines the natural frequency, has a large impact on the effectiveness of the system. L_{ee} is a direct function of α. Because of the large area of the platform, α is given a lenient constraint to allow the TLCD to closely tune to the necessary natural frequency. The TLCD is constrained to having an $\alpha \leq 10$.
6. Similar to the nacelle constraint, ζ is set between $0 < \zeta \leq 500$.
7. The constraints on A are also relaxed due to the large size of the platform and increased mass values of the TLCD. Aesthetics don't play a part in determining the TLCD shape because it will mostly be hidden underwater. It is therefore decided to make $A \leq 15$ m^2 and $A \geq 0.05$ m^2.

$1 \text{ m} < B < 45 \text{ m}$	Defined by platform dimensions
$max\|w\| \leq \left[\frac{L-B}{2}\right] * 0.9$	Maximum water displacement cannot exceed height of vertical TLCD column with safety factor
$\frac{L-B}{2} < 5.5\ m, \frac{L-B}{2} > 0.5\ m$	Set according to barge dimensions and vertical water displacement values
$1 \text{ m} < L \leq 56 \text{ m}$	Set according to barge dimensions and vertical water displacement values
$0.1 \leq \alpha \leq 10$	Wide range to accommodate possibly large TLCD areas
$0 < \zeta \leq 500$	Set wide range of ζ
$0.05 \text{ m}^2 \leq A \leq 15 \text{ m}^2$	Increased size due to large platform and increased TLCD mass

Table 7.3: Table showing summary of barge platform TLCD dimensional constraints

7.2.4 Spar Platform Constraints

The options of using a spar radius of 3 m and 6 m are explored. This makes a few of the constraints have different values according to the different radii. The circular shape of the spar imposes a unique space constraint on the possibility of sizing an optimally designed TLCD for the platform. Because of the small spar radius, it is important to

maximize the space used by a TLCD. This involves modifying the TLCDs shape. The goal is to design a TLCD with semi-circular vertical cross-sectional area columns so that they can mesh with the inside wall of the spar. A top and isometric image of a TLCD's overall design incorporated into the spar is shown in Figure 7.3.

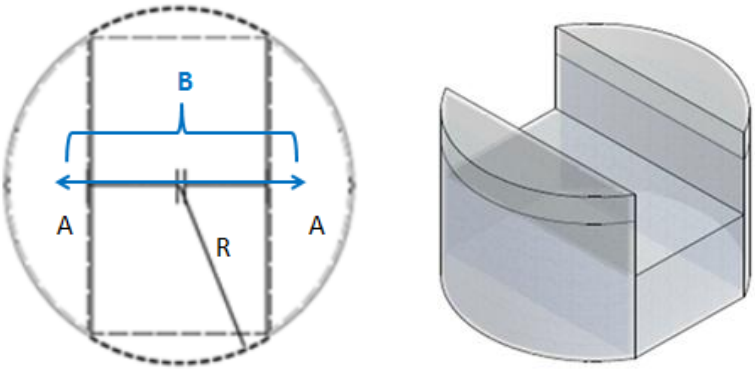

Figure 7.3: Top and isometric view of TLCD design within a spar platform

The following considerations are used when designing a TLCD for the spar platform:

1. The horizontal length of the TLCD, *B* must be within the restrictions set by the spar radius. For a radius of 3 m, this limits *B* to be less than 6 m. For a radius of 6 m, this limits B to be less than 12 m.
2. A single vertical column must have a cross-sectional area *A* that is smaller than half of the cross-sectional area of the circular spar.
3. Because of the semi-circular shape of *A*, the value of *A* must be somehow dependent on *B*. It is decided that the end points of *B* will be located 1/3 of the distance within *A* from the inside edge of the TLCD as shown in the Figure 7.4. This allows *A* to be defined as a function of *B*.
4. The vertical water travel is constrained according to $max|w| \leq \left[\frac{L-B}{2}\right] * 0.9$.

5. Though the spar is extremely long and somewhat empty, a TLCD cannot take up all of the space. The spar must be partially empty to provide buoyancy and must hold the ballast, which could potentially occupy a large amount of space. Because of this reason, the TLCD length of a spar with R = 3 m is constrained to be less than 46 m. For R = 6 m, the TLCD length must be less than 52 m. This would give a maximum TLCD height of 20 m at equilibrium. The water displacement range of motion can be: $w \approx \mp\left(\frac{20m}{2}\right) * 0.9 = 9m$. Because L is given a lower boundary of 2 m, the vertical column height constraint range is then defined to be between 20 m and 2 m.
6. Because of the spar's low natural frequency, it is determined that A will not need to be large because it won't experience a large amount of water motion. Therefore, most of the water mass will be located in the horizontal column of the TLCD. This would lead to a large value of $A1$, which would produce a small α. The constraint on α is set so that $.02 \leq \alpha \leq 5$.
7. Though the results of $A1$ may be large due to the small value of α, it must be constrained by the available vertical length of the spar. Similar to the constraints set on A, the value of $A1$ is defined to be less than $\pi R^2/2$ based on the radius of the spar.
8. Similar to before, ζ is set between $0 < \zeta \leq 500$.

1 m $< B < 2R$	Defined by spar dimensions
$A < (\pi R^2)/2$	Single vertical column cannot be larger than half of spar area
$A = f(B)$	The end points of B are defined by A
$\lvert w \rvert \leq \left[\frac{L-B}{2}\right] * 0.9$	Maximum water displacement cannot exceed height of vertical TLCD column with safety factor
$\frac{L-B}{2} < 20, \frac{L-B}{2} > 1$	Set according to spar dimensions and vertical water displacement values
For R = 3 m, 2 m < L < 46 m For R = 6 m, 2 m < L < 52 m	Set according to spar dimensions and vertical water displacement values
$0.02 \leq \alpha \leq 5$	Small values because of increased platform frequency
$A1 < (\pi R^2)/2$	Reasonable values set by available vertical area in spar
$0 < \zeta \leq 500$	Set wide range of ζ

Table 7.4: Table showing summary of spar platform TLCD dimensional constraints

CHAPTER 8

OPTIMIZATION RESULTS

8.1 Organizing Results

The optimization results can be grouped according to the following:

- Type of OWT (monopile, barge, spar buoy).
- Location of the TLCD (nacelle, platform when applicable).
- Testing method performed (initial perturbation or external force).
- Non-uniform or uniform TLCD: The non-uniformity of the cross-sectional areas of a TLCD can add complexity to the construction and installation of a TLCD in an OWT. It is therefore interesting to optimize a uniform TLCD with α = 1 and compare its effectiveness to that of a non-uniform cross-sectional area TLCD. This simplistic design approach can speed build time and increase the ease of manufacturing.
- TLCD mass values: Mass ratio values of approximately 2% of a structure's overall mass are typically used when designing a TMD or TLCD. For this thesis, values that equate to approximately 1%, 2% and 4% will be used. This is done to test the effectiveness of each mass value while observing their corresponding TLCD dimensional and performance differences. When examining the monopile OWT, these values equate approximately to 10,000 kg, 20,000 kg and 40,000 kg. For scenarios when the TLCD is placed in the platform, values of 100,000 kg, 200,000 kg and 400,000 kg are used to represent approximately 1%, 2% and 4% of the platforms entire floating mass.

- Damping and stiffness: Stewart has generated ideal TMD's using models similar to those explained in this thesis. Comparisons are made between the equivalent stiffness, $k_{eq,TLCD}$, and the equivalent damping, $d_{eq,TLCD}$, values generated by the simulations using a TLCD and those found in Stewart's thesis for a TMD (k_{TMD}, d_{TMD}). The comparisons to Stewart's results are examined in Chapter 8.4 when applicable. Otherwise, the values are shown in Chapter 8.1 – 8.3.

  The equivalent TLCD stiffness, $k_{eq,TLCD}$, can be found by using the equation for the TLCD natural frequency $\left(\omega_{TLCD} = \sqrt{2g/L_{ee}}\right)$, equating it to the natural frequency of an arbitrary mass-spring system $\left(\omega_{TLCD} = \sqrt{k_{eq}/m_{TLCD}}\right)$ and solving for the equivalent stiffness value. The TLCD equivalent damping term is included in each DOF containing a TLCD and is defined as $d_{eq,TLCD} = (\rho A B R_{TLCD} \zeta / 2L_{ee})|\dot{w}|\dot{w}$. The damping term can be found in the EOMs for the DOF of each system which contains a TLCD (Eqn. (6.2), (6.4), (6.8)). This term is non-linear because of the squared velocity term. The equivalent damping term can be solved for by linearizing this term. Equivalent damping and stiffness values are derived for both the initial perturbation and external forcing methods. When applicable, the ideal TMD values are compared to the values generated by the external forcing method because they were also derived under realistic forcing conditions.

This chapter will examine the results of all of the scenarios described above and compare them to a baseline simulation of an OWT that does not contain a TLCD. For the non-uniform TLCD subjected to the external forcing method, comparisons of the tower top reduction and platform motion reduction are made to the values generated by Stewart

for a similar system with an ideal TMD displaced in the fore-aft direction. This will help to determine whether a TLCD or TMD system would be more appropriate for different OWT scenarios when subjected to a realistic forcing function.

8.2 Monopile

8.2.1 Monopile - Initial Perturbation

This section presents the optimum values found for the monopile when subjected to an initial perturbation for a non-uniform and uniform TLCD. Optimum values of the independent parameters of the TLCD and the reduction in monopile motion, as well as the baseline comparison can be seen in Table 8.1.

		Non-uniform ($\alpha \neq 1$)			Uniform ($\alpha = 1$)		
TLCD Mass (kg)	0 (Baseline, No TLCD)	10,000	20,000	40,000	10,000	20,000	40,000
α	0	0.41	0.39	0.39	1	1	1
A (m^2)	0	0.22	0.42	0.83	0.48	0.95	1.91
A1 (m^2)	0	0.54	1.08	2.15	0.48	0.95	1.91
B (m)	0	16	16	16	16	16	16
L (m)	0	22.09	22.40	22.79	21.0	21.0	21.0
Lee (m)	0	12.59	12.69	13.02	21.0	21.0	21.0
ζ	0	12.88	11.48	9.70	58.67	61.0	61.0
$k_{eq,TLCD}$ (N/m)	0	15,583	30,927	60,295	9,336	18,680	37,370
$d_{eq,TLCD}$ (Ns/m)	0	3.24e5	5.52e5	8.95e5	1.91e6	3.98e6	7.97e6
St.Dev.TTD (m)	0.472	0.292	0.227	0.173	0.366	0.308	0.246
St.Dev.TTD % Reduction	-	38.18%	51.82%	63.32%	22.49%	34.80%	47.87%
St.Dev.wDisp (m)	0	0.98	0.82	0.66	0.32	0.27	0.22
Max.wDisp (m)	0	2.61	2.70	2.72	0.72	0.71	0.70

Table 8.1: Table showing initial perturbation optimum results for non-uniform and uniform cross-sectional area TLCD attached to monopile nacelle

The non-uniform TLCD results show that the use of an optimally sized TLCD produces significant tower top vibration reduction when the TLCD is placed in the nacelle of a monopile wind turbine. Many conclusions can be drawn from these results.

By increasing the mass of the TLCD, a higher value of tower top vibration

reduction is achieved. As the TLCD mass increases, the increase in vibration reduction is not strongly dependent on *L*, but rather the cross-sectional areas of the TLCD. By increasing the liquid mass of the TLCD, the TLCD cross-sectional areas increase in size to accommodate more liquid mass. Though α stays relatively constant for each analysis, *A* and *A1* double in size as the mass is doubled for each successive case.

It is noticed that with the increase in m_{TLCD}, the St.Dev.TTD decreases. This is because the TLCD is having a greater effect on the motion of the tower. Max.wDisp stays about the same, but as the tower motion decreases, the water motion decreases as well. This is why St.Dev.TTD is lower.

The values for ζ also stay within a certain range. This defines the orifice size and produces a specific amount of viscous damping appropriate for the system.

A uniform TLCD can also be optimized when placed in a monopile nacelle. Along with $\alpha = 1$, *B* is fixed at 16 m similar to the non-uniform TLCD. Other constraints remained similar according to Table 7.2. Table 8.1 shows that TLCDs with uniform cross-sectional areas underperform those with non-uniform cross-sectional areas of the same length. To perform the same as a TLCD with non-uniform cross-sectional area, a TLCD with uniform cross-sectional area would have to have greater *B* and *L* values, or a greater mass. Due to the constraints of the problem, increasing *B* and *L* to produce similar reductions in St.Dev.TTD to that of a non-uniform cross-sectional area TLCD is not a practical option. Thus a TLCD with non-uniform cross-sectional area ratio can greatly reduce the length requirement of a TLCD with a uniform cross-sectional area in suppressing the same level of vibration. This corresponds with information presented by Gao et al. [10].

8.2.2 Monopile - External Forcing

TLCD Mass (kg)	0 (Baseline, No TLCD)	Non-uniform ($\alpha \neq 1$)			Uniform ($\alpha = 1$)		
		10,000	20,000	40,000	10,000	20,000	40,000
α	0	0.31	0.32	0.36	1	1	1
A (m^2)	0	0.17	0.36	0.80	0.47	0.95	1.90
A1 (m^2)	0	0.57	1.13	2.24	0.47	0.95	1.90
B (m)	0	16	16	16	16	16	16
L (m)	0	21.35	21.16	21.18	21.43	21.04	21.03
Lee (m)		10.26	10.30	10.87	21.43	21.04	21.03
ζ	0	10.83	10.34	8.12	83.23	82.70	86.94
St.Dev.TTD (m)	0.053	0.050	0.049	0.047	0.052	0.052	0.051
TLCD St.Dev.TTD % Reduction	-	4.12%	6.92%	9.91%	0.53%	1.21%	2.62%
Optimal TMD TTD % Reduction	-	5.70%	6.20%	8.90%	-	-	-
St.Dev.wDisp (m)	0	0.34	0.31	0.27	0.06	0.06	0.06
Max.wDisp (m)	0	2.27	2.21	2.18	0.43	0.43	0.42

Table 8.2: Table showing external forcing optimum results for non-uniform and uniform cross-sectional area TLCD attached to monopile nacelle

The monopile is subjected to a purely aerodynamic thrust force. The TLCD reduces St.Dev.TTD in all cases, but the non-uniform TLCD significantly outperforms the uniform TLCD. L_{ee} stays relatively constant to produce a TLCD natural frequency that effectively damps out the natural frequency of the tower. It is interesting to note the grouping of the values for ζ in each case.

The non-uniform optimized TLCD produces TTD reduction values that are quite similar to that of the optimal TMD generated by Stewart, while the higher mass values produce even more TTD reduction than the TMD.

8.3 Barge

8.3.1 Barge Nacelle - Initial Perturbation

This section presents the optimum values found for the barge when subjected to an initial perturbation for a non-uniform and a uniform TLCD. Optimum values of the

independent parameters of a non-uniform TLCD and the reduction in barge St.Dev.TTD and St.Dev.PlatPitch can be seen in Table 8.3.

		Non-uniform (α ≠ 1)			Uniform (α = 1)		
TLCD Mass (kg)	0 (Baseline, No TLCD)	10,000	20,000	40,000	10,000	20,000	40,000
α	0	0.45	0.45	0.44	1	1	1
A (m^2)	0	0.24	0.47	0.93	0.48	0.95	1.90
A1 (m^2)	0	0.53	1.05	2.10	0.48	0.95	1.90
B (m)	0	16	16	16	16	16	16
L (m)	0	22.87	22.93	22.92	21	21	21
Lee (m)	0	13.99	14.12	14.03	21	21	21
ζ	0	68.25	61.12	65.33	123.73	121.49	129.86
$k_{eq,TLCD}$ (N/m)	0	14,023	27,797	55,957	9,342	18,685	37,365
$d_{eq,TLCD}$ (Ns/m)	0	4.07e6	2.95e6	6.29e6	4.07e6	7.99e6	1.71e7
St.Dev.TTD (m)	0.365	0.349	0.335	0.315	0.352	0.341	0.322
St.Dev.TTD % Reduction	-	4.56%	8.30%	13.76%	3.62%	6.74%	11.64%
St.Dev.PlatPitch (°)	1.595	1.554	1.485	1.407	1.532	1.475	1.385
St.Dev.PlatPitch % Reduction	-	2.61%	6.91%	11.78%	3.98%	7.52%	13.18%
St.Dev.wDisp (m)	0	1.43	1.44	1.37	0.73	0.71	0.66
Max.wDisp (m)	0	3.08	3.11	3.11	1.52	1.51	1.47

Table 8.3: Table showing initial perturbation optimum results for non-uniform and uniform cross-sectional area TLCD attached to barge nacelle

The simulation of the barge includes the platform DOF. Similar to the St.Dev.TTD, it has a baseline value when the barge does not contain a TLCD. As shown, increasing the mass of the TLCD does increase the overall reduction in St.Dev.TTD as well as the St.Dev.PlatPitch. Similar to the monopile, α tends to stay relatively constant as the cross-sectional areas of the TLCD essentially double to accommodate a doubling mass in each successive case for a non-uniform TLCD. L_{ee} also stays relatively constant, defining the natural frequency of the TLCD to be a relatively constant value.

The use of a non-uniform TLCD produces larger St.Dev.TTD % reduction than a uniform TLCD. The value of L is equal to the lower boundary of L set by the constraints of the nacelle. Once again, the uniformity of the TLCD within constraints set by the nacelle is restricting the potential of reducing St.Dev.TTD. One interesting point is how the use of a uniform TLCD slightly increases the St.Dev.PlatPitch % Reduction for each

optimized case compared to a non-uniform TLCD. This is due to the lower natural frequency of the uniform TLCD as defined by its value of L_{ee}. This makes it more effective at reducing the low natural frequency of the platform.

8.3.2 Barge Nacelle - External Forcing

		Non-uniform ($\alpha \neq 1$)			Uniform ($\alpha = 1$)		
TLCD Mass (kg)	0 (Baseline, No TLCD)	10,000	20,000	40,000	10,000	20,000	40,000
α	0	5.23	5.28	5.19	1	1	1
A (m^2)	0	1.00	2.23	4.25	0.437	0.871	1.74
A1 (m^2)	0	0.19	0.42	0.83	0.437	0.871	1.74
B (m)	0	16	16	16	16	16	16
L (m)	0	22.99	21.95	22.34	22.87	22.95	22.93
Lee (m)	0	90.63	90.35	89.43	22.87	22.95	22.93
ζ	0	3.71	5.52	4.34	75.53	62.57	64.80
St.Dev.TTD (m)	0.380	0.376	0.372	0.366	0.380	0.380	0.380
TLCD St.Dev.TTD % Reduction	-	1.06%	2.03%	3.79%	-0.06%	-0.11%	-0.24%
Optimal TMD TTD % Reduction	-	5.90%	11.00%	15.60%	-	-	-
St.Dev.PlatPitch (°)	1.973	1.952	1.931	1.892	1.960	1.948	1.924
St.Dev.PlatPitch % Reduction	-	1.08%	2.12%	4.12%	0.63%	1.26%	2.46%
St.Dev.wDisp (m)	0	1.43	1.20	1.28	1.04	1.09	1.07
Max.wDisp (m)	0	3.06	2.64	2.80	2.74	2.92	2.86

Table 8.4: Table showing external forcing optimum results for non-uniform and uniform cross-sectional area TLCD attached to barge nacelle

When subjected to an aerodynamic thrust force and a hydrodynamic pitching moment, a non-uniform TLCD reduces both St.Dev.TTD and St.Dev.PlatPitch. However, a uniform TLCD actually increases TTD for each mass. This shows that the uniform TLCD cannot be tuned properly within the constraints of the nacelle to damp out tower motion. In this case, the TLCD is essentially only acting as added weight to the nacelle.

A non-uniform TLCD located in the barge nacelle underperforms considerably compared to the optimal TMD. This is due to restrictions placed on the TLCD. In Stewart's simulations, stops are imposed so that the TMD mass is allowed to nonlinearly strike the walls of the platform. This allowed more area for movement of the mass, which

increases overall TTD reduction. Stops are not imposed for the TLCD and the water is not allowed to be displaced beyond a given constraint. Given a larger area to occupy (or possibly with the implementation of stops), the TLCD would be able increase its displacement reduction capabilities, making it more comparable to the TMD.

8.3.3 Barge Platform - Initial Perturbation

		Non-uniform ($\alpha \neq 1$)			Uniform ($\alpha = 1$)		
TLCD Mass (kg)	0 (Baseline, No TLCD)	100,000	200,000	400,000	100,000	200,000	400,000
α	0	1.43	1.44	1.39	1	1	1
A (m^2)	0	2.50	4.98	9.75	1.79	3.58	7.15
A1 (m^2)	0	1.75	3.47	7.01	1.79	3.58	7.15
B (m)	0	42.95	44.27	44.53	44.99	44.95	44.97
L (m)	0	54.88	53.58	53.54	55.83	55.91	55.95
Lee (m)	0	71.22	72.88	70.95	55.83	55.91	55.95
ζ	0	3.24	5.68	14.83	11.43	15.54	29.09
$k_{eq,TLCD}$ (N/m)	0	27,548	53,842	1.11e5	35,143	70,180	1.40e5
$d_{eq,TLCD}$ (Ns/m)	0	48,864	1.72e5	9.08e5	1.65e5	4.47e5	1.67e6
St.Dev.TTD (m)	0.365	0.310	0.291	0.278	0.337	0.317	0.291
St.Dev.TTD % Reduction	-	15.02%	20.20%	23.77%	7.70%	13.21%	20.25%
St.Dev.PlatPitch (°)	1.595	1.180	1.005	0.888	1.405	1.261	1.066
St.Dev.PlatPitch % Reduction	-	26.01%	36.98%	44.33%	11.93%	20.98%	33.17%
St.Dev.wDisp (m)	0	2.09	1.48	0.86	1.39	1.17	0.84
Max.wDisp (m)	0	4.14	3.31	2.44	3.38	3.06	2.56

Table 8.5: Table showing initial perturbation optimum results for non-uniform and uniform cross-sectional area TLCD attached to barge platform

A uniform TLCD is not quite as effective as the non-uniform TLCD, but it does however provide significant St.Dev.TTD and St.Dev.PlatPitch reduction and could be examined for design simplicity. The one main difference in this simulation compared to placing a TLCD in the nacelle is that the TLCD dimensions are allowed more freedom. This includes allowing *B* to be as small as 1 m and *L* to be as small as 3 m. However, the results show that B is once again close to the upper boundary of the constraint, proving that having a TLCD with a large horizontal length increases overall effectiveness.

The obvious advantage to placing a TLCD in the platform of the barge is that it has the ability to contain a much larger mass. As shown, placing a TLCD in the platform reduces the St.Dev.PlatPitch by up to 44%. Due to the coupling between the platform and tower motion, St.Dev.TTD is reduced as well.

8.3.4 Barge Platform - External Forcing

		Non-uniform ($\alpha \neq 1$)			Uniform ($\alpha = 1$)		
TLCD Mass (kg)	0 (Baseline, No TLCD)	100,000	200,000	400,000	100,000	200,000	400,000
α	0	2.19	1.87	1.97	1	1	1
A (m^2)	0	3.38	6.01	13.66	1.82	3.57	7.20
A1 (m^2)	0	1.75	3.22	6.92	1.82	3.57	7.20
B (m)	0	35.31	41.72	38.60	44.54	45.00	44.98
L (m)	0	45.32	52.65	48.32	54.82	55.97	55.59
Lee (m)	0	87.48	88.86	85.92	54.82	55.97	55.59
ζ	0	3.38	2.79	4.48	16.43	9.61	15.89
St.Dev.TTD (m)	0.378	0.373	0.366	0.360	0.376	0.373	0.366
St.Dev.TTD % Reduction	-	1.89%	3.62%	5.29%	0.93%	1.92%	3.70%
St.Dev.PlatPitch (°)	1.973	1.926	1.885	1.853	1.959	1.948	1.922
St.Dev.PlatPitch % Reduction	-	2.37%	4.43%	6.06%	0.68%	1.26%	2.59%
St.Dev.wDisp (m)	0	1.72	2.00	1.46	1.38	1.62	1.37
Max.wDisp (m)	0	4.15	4.90	3.85	4.16	4.88	4.20

Table 8.6: Table showing external forcing optimum results for non-uniform and uniform cross-sectional area TLCD attached to barge platform

The large area of the platform area of the barge allows the TLCD's dimensions to be optimized over a wide range of values. Though the non-uniform TLCD is the most effective, both the non-uniform and uniform TLCDs prove to be effective in reducing the St.Dev.PlatPitch of the barge. Given the coupling between the platform and tower motion, this translates into added reduction in St.Dev.TTD for a properly tuned TLCD. As shown, L_{ee} is very large. This equates to a low TLCD natural frequency, which has more of an effect on the barge platform.

8.4 Spar Buoy

8.4.1 Spar Nacelle - Initial Perturbation

TLCD Mass (kg)	0 (Baseline, No TLCD)	Non-uniform (α ≠ 1)			Uniform (α = 1)		
		10,000	20,000	40,000	10,000	20,000	40,000
α	0	0.39	0.41	0.39	1	1	1
A (m^2)	0	0.21	0.45	0.84	0.48	0.95	1.91
A1 (m^2)	0	0.55	1.09	2.17	0.48	0.95	1.91
B (m)	0	16	16	16	16	16	16
L (m)	0	22.02	21.77	22.18	21.00	21.00	21.00
Lee (m)	0	12.21	12.39	12.38	21.00	21.00	21.00
ζ	0	36.37	33.12	25.64	203.21	208.84	210.82
$k_{eq,TLCD}$ (N/m)	0	16,067	31,672	63,373	9,343	18,686	37,371
$d_{eq,TLCD}$ (Ns/m)	0	8.17e5	1.55e6	2.25e6	5.94e6	1.22e7	2.47e7
St.Dev.TTD (m)	0.203	0.138	0.118	0.102	0.162	0.142	0.123
St.Dev.TTD % Reduction	-	32.20%	42.06%	49.58%	20.08%	29.99%	39.55%
St.Dev.PlatPitch (°)	1.989	1.989	1.989	1.988	1.989	1.989	1.987
St.Dev.PlatPitch % Reduction	-	0.04%	0.06%	0.09%	0.04%	0.08%	0.14%
St.Dev.wDisp (m)	0	0.86	0.79	0.83	0.31	0.31	0.31
Max.wDisp (m)	0	2.66	2.57	2.74	0.85	0.84	0.83

Table 8.7: Table showing initial perturbation optimum results for non-uniform and uniform cross-sectional area TLCD attached to spar nacelle

Table 8.7 shows results for a non-uniform and uniform TLCD in the nacelle of the spar buoy. The results are promising for reducing St.Dev.TTD, with reductions up to 49%. The TLCD is able to tune to the tower natural frequency, providing ample reduction. Given the nature and design of the spar platform, it has an extremely large pitching moment of inertia in the fore-aft direction, which contributes to its high resistance to motion and its low natural frequency. For this reason, the TLCD does little to reduce the St.Dev.PlatPitch.

The uniform TLCD has a smaller effect on the St.Dev.TTD due to its pre-defined natural frequency given by the value of L_{ee} and just about the same negligible effect on the St.Dev.PlatPitch.

8.4.2 Spar Nacelle - External Forcing

TLCD Mass (kg)	0 (Baseline, No TLCD)	Non-uniform (α ≠ 1)			Uniform (α = 1)		
		10,000	20,000	40,000	10,000	20,000	40,000
α	0	0.51	2.98	2.74	1	1	1
A (m^2)	0	0.27	1.66	0.79	0.44	0.91	1.74
A1 (m^2)	0	0.52	0.56	0.29	0.44	0.91	1.74
B (m)	0	16	16	16	16	16	16
L (m)	0	22.10	22.66	22.76	22.86	22.05	22.98
Lee (m)	0	14.26	54.29	50.63	22.86	22.05	22.98
ζ	0	121.34	126.60	131.55	270.32	273.75	285.38
St.Dev.TTD (m)	0.0760	0.0761	0.0761	0.0762	0.0761	0.0762	0.0763
TLCD St.Dev.TTD % Reduction	-	-0.03%	-0.06%	-0.14%	-0.06%	-0.15%	-0.33%
Optimal TMD TTD % Reduction	-	1.9%	4.4%	8.4%	-	-	-
St.Dev.PlatPitch (°)	1.723	1.720	1.722	1.720	1.721	1.720	1.718
St.Dev.PlatPitch % Reduction	-	0.13%	0.06%	0.15%	0.09%	0.14%	0.25%
St.Dev.wDisp (m)	0	0.55	0.10	0.11	0.29	0.29	0.29
Max.wDisp (m)	0	1.71	0.35	0.41	0.88	0.88	0.88

Table 8.8: Table showing external forcing optimum results for non-uniform and uniform cross-sectional area TLCD attached to spar nacelle

The TLCD actually has a negative effect on the St.Dev.TTD. Constraints set by the nacelle size prevent the TLCD from tuning properly to damp out tower motion. This is seen in the erratic values produced by the optimization for terms such as α and L_{ee} as the optimization routine is struggling to find values that produce positive results. Similar to the uniform TLCD for the barge nacelle under thrusting conditions, the extra tower top mass from the mistuned TLCD only causes more bending due to gravitational and inertial pitching. Also, the rotor thrust leads to a large non-zero mean platform pitch, which causes the tower as well as the TLCD to tilt. This causes gravity to pull water in the TLCD to one side. The large values of ζ are used to keep the max water displacement low so that water does not completely drain to one side. Results show that placing a TLCD in the nacelle of the spar will add no performance enhancement.

8.4.3 Spar Platform - Initial Perturbation

Table 8.9 shows the results for a non-uniform and uniform TLCD with R = 3 and Table 8.10 shows the results for a non-uniform and uniform TLCD with R = 6.

		Non-uniform (α ≠ 1)			Uniform (α = 1)		
TLCD Mass (kg)	0 (Baseline, No TLCD)	100,000	200,000	400,000	100,000	200,000	400,000
α	0	0.30	0.36	0.63	1	1	1
A (m^2)	0	4.22	5.15	8.88	13.95	12.39	13.03
A1 (m^2)	0	14.14	14.14	14.14	13.95	12.39	13.03
B (m)	0	4.35	4.10	3.19	2.04	2.39	2.23
L (m)	0	13.53	31.78	43.16	7.17	16.14	30.71
Lee (m)	0	10.48	29.19	41.98	7.17	16.14	30.71
ζ	0	283.67	185.43	224.02	36.92	129.89	297.28
$k_{eq,TLCD}$ (N/m)	0	1.87e5	1.34e5	1.87e5	2.74e5	2.43e5	2.56e5
$d_{eq,TLCD}$ (Ns/m)	0	5.85e7	1.75e7	1.78e7	1.73e7	2.81e7	3.31e7
St.Dev.TTD (m)	0.203	0.203	0.203	0.203	0.203	0.203	0.203
St.Dev.TTD % Reduction	-	0.22%	0.12%	0.08%	0.14%	0.10%	-0.02%
St.Dev.PlatPitch (°)	1.989	1.994	2.000	2.011	1.994	2.000	2.011
St.Dev.PlatPitch % Reduction	-	-0.22%	-0.49%	-1.08%	-0.24%	-0.51%	-1.09%
St.Dev.wDisp (m)	0	0.21	0.17	0.08	0.03	0.04	0.04
Max.wDisp (m)	0	0.58	0.55	0.30	0.15	0.15	0.14

Table 8.9: Table showing initial perturbation optimum results for non-uniform and uniform cross-sectional area TLCD attached to spar platform when R = 3

It was determined that it could be possible to design a spar with a larger radius to house a TLCD if the TLCD proved to be efficient enough. For this reason, the option of using a spar section that has a radius of 6 m was also explored so that the differences could be measured. Due to the size constraints set by the spar platform, an optimized TLCD provides little, if any motion reduction capabilities to the tower top. The platform is also experiencing increased motion due to the presence of the TLCD. Also because of the small spar radius, the TLCD is not able to size properly to reduce St.Dev.PlatPitch. When examining the non-uniform TLCD, it is found that each optimized value of *A1* is equal to the constraint $(\pi R^2)/2$. Increasing m_{TLCD} while keeping *A1* at its constraint lowers the effectiveness of the TLCD.

TLCD Mass (kg)	0 (Baseline, No TLCD)	Non-uniform (α ≠ 1)			Uniform (α = 1)		
		100,000	200,000	400,000	100,000	200,000	400,000
α	0	0.29	0.29	0.43	1	1	1
A (m^2)	0	2.35	5.09	18.28	9.32	23.41	56.55
A1 (m^2)	0	8.20	17.37	42.92	9.32	23.41	56.55
B (m)	0	11.13	10.55	8.50	9.81	7.83	4.00
L (m)	0	14.78	13.84	10.42	10.73	8.54	7.08
Lee (m)	0	6.90	6.38	5.54	10.73	8.54	7.08
ζ	0	96.20	62.50	72.05	486.14	481.52	489.52
$k_{eq,TLCD}$ (N/m)	0	2.84e5	6.15e5	1.41e6	1.83e5	4.593e	1.11e6
$d_{eq,TLCD}$ (Ns/m)	0	4.30e7	6.21e7	2.38e8	4.89e8	1.22e9	1.85e9
St.Dev.TTD (m)	0.203	0.201	0.197	0.190	0.202	0.201	0.201
St.Dev.TTD % Reduction	-	1.29%	2.86%	6.32%	0.57%	1.23%	1.01%
St.Dev.PlatPitch (°)	1.989	1.993	1.997	2.007	1.993	1.997	2.010
St.Dev.PlatPitch % Reduction	-	-0.14%	-0.34%	-0.84%	-0.16%	-0.38%	-1.02%
St.Dev.wDisp (m)	0	0.55	0.52	0.29	0.14	0.11	0.06
Max.wDisp (m)	0	1.51	1.41	0.85	0.39	0.31	0.16

Table 8.10: Table showing initial perturbation optimum results for non-uniform and cross-sectional area TLCD attached to spar platform when R = 6

Given the size of the TLCD mass values used and the small area constraints, the spring constants are incredibly high and provide little to damp the low frequency of the platform. The TLCD cannot be tuned to a frequency that is low enough to reduce motion brought on by the low frequency of the platform. The liquid motion within the TLCD is moving faster than that of the platform, causing the platform to move slightly more. In this case, the TLCD is not effective and it's only adding to the motion of the platform. With the case of the non-uniform TLCD, The St.Dev.TTD improves considerably, while the St.Dev.PlatPitch results for both the non-uniform and uniform TLCD are improved with the increase in spar radius. It is interesting to see how the St.Dev.TTD % reduction increases and reduces with the increase in m_{TLCD} for a uniform TLCD. For the case of m_{TLCD} = 400,000 kg, it would be expected that the St.Dev.TTD % would increase with increasing mass value. This however is not the case. As m_{TLCD} increases, the value for *A1* reaches the constraint$(\pi R^2)/2$, which makes adding anymore mass to the TLCD useless.

8.4.4 Spar Platform - External Forcing

Similar to the initial perturbation test, spar buoys with radii of 3 m and 6 m were tested under conditions of aerodynamic thrust and hydrodynamic pitching. The results are shown for the different spar radii in Table 8.11 and Table 8.12, respectively.

		Non-uniform ($\alpha \neq 1$)			Uniform ($\alpha = 1$)		
TLCD Mass (kg)	0 (Baseline, No TLCD)	100,000	200,000	400,000	100,000	200,000	400,000
α	0	0.79	2.30	2.67	1	1	1
A (m^2)	0	5.52	8.28	11.56	9.09	11.12	9.91
A1 (m^2)	0	6.98	3.60	4.34	9.09	11.12	9.91
B (m)	0	4.00	3.33	2.57	3.14	2.67	2.98
L (m)	0	17.05	26.03	36.20	11.00	17.99	40.36
Lee (m)	0	16.22	30.36	40.49	11.00	17.99	40.36
ζ	0	226.80	53.22	204.63	92.72	221.83	23.59
St.Dev.TTD (m)	0.0760	0.0755	0.0750	0.0741	0.0755	0.0750	0.0741
TLCD St.Dev.TTD % Reduction	-	0.69%	1.33%	2.59%	0.73%	1.34%	2.56%
Optimal TMD TTD % Reduction	-	0.7%	1.6%	-0.3%	-	-	-
St.Dev.PlatPitch (°)	1.723	1.703	1.686	1.656	1.703	1.686	1.657
St.Dev.PlatPitch % Reduction	-	1.17%	2.14%	3.85%	1.15%	2.14%	3.84%
St.Dev.wDisp (m)	0	0.06	0.02	0.01	0.04	0.04	0.05
Max.wDisp (m)	0	0.23	0.08	0.05	0.14	0.12	0.16

Table 8.11: Table showing external forcing optimum results for non-uniform and uniform cross-sectional area TLCD attached to spar platform when R = 3

When applying realistic forcing, the TLCD does provide some St.Dev.TTD % reduction and St.Dev.PlatPitch % reduction. Both the uniform and non-uniform TLCD produce about the same amount of both St.Dev.TTD and St.Dev.PlatPitch % reduction for each different mass value. It is interesting to note how the optimization routine finds optimal values for variables such as L as m_{TLCD} increases. For each case of increasing m_{TLCD}, the value for L increases considerably to accommodate for the mass. This shows that there is a threshold value for m_{TLCD} where L becomes the most important variable for TLCD definition.

TLCD Mass (kg)	0 (Baseline, No TLCD)	Non-uniform ($\alpha \neq 1$)			Uniform ($\alpha = 1$)		
		100,000	200,000	400,000	100,000	200,000	400,000
α	0	0.26	0.14	0.04	1	1	1
A (m^2)	0	2.11	2.27	1.33	3.13	13.04	50.27
A1 (m^2)	0	8.05	15.86	30.86	3.13	13.04	50.27
B (m)	0	11.20	11.62	11.42	10.98	9.24	4.70
L (m)	0	15.86	21.29	47.37	31.93	15.34	7.96
Lee (m)	0	7.60	11.73	36.44	31.93	15.34	7.96
ζ	0	242.90	287.81	296.70	32.61	297.42	245.51
St.Dev.TTD (m)	0.0760	0.0755	0.0749	0.0733	0.0755	0.0750	0.0741
TLCD St.Dev.TTD % Reduction	-	0.77%	1.57%	3.58%	0.77%	1.38%	2.61%
St.Dev.PlatPitch (°)	1.723	1.701	1.681	1.636	1.702	1.684	1.656
St.Dev.PlatPitch % Reduction	-	1.27%	2.45%	5.02%	1.19%	2.24%	3.87%
St.Dev.wDisp (m)	0	0.53	0.95	2.98	0.15	0.12	0.06
Max.wDisp (m)	0	1.91	3.45	10.80	0.62	0.42	0.21

Table 8.12: Table showing external forcing optimum results for non-uniform and uniform cross-sectional area TLCD attached to spar platform when R = 6

Once again, increasing spar radius to 6 m does increase TLCD effectiveness, but only by fractions of a percent as judged by the St.Dev.TTD and St.Dev.PlatPitch. In order for any large improvement to take place, the constraints set by the spar would have to open considerably. This would include increasing the spar radius even further so that the TLCD dimensions would be given room to expand where necessary.

8.5 Summary of Results

The St.Dev.TTD and St.Dev.PlatPitch reduction values for different OWT models that are coupled with non-uniform TLCDs subjected to the external forcing method are summarized in Table 8.13. This gives a clear representation as to which scenarios an OWT coupled with a TLCD may be beneficial when it is subjected to realistic external conditions.

OWT	TMD/TLCD Mass (kg)	Location	St.Dev.TTD % Reduction	St.Dev.PlatPitch % Reduction
Monopile	10,000	Nacelle	4.12%	-
Monopile	20,000	Nacelle	6.92%	-
Monopile	40,000	Nacelle	9.91%	-
Barge	10,000	Nacelle	1.06%	1.08%
Barge	20,000	Nacelle	2.03%	2.12%
Barge	40,000	Nacelle	3.79%	4.12%
Barge	100,000	Platform	1.89%	2.37%
Barge	200,000	Platform	3.62%	4.43%
Barge	400,000	Platform	5.29%	6.06%
Spar	10,000	Nacelle	-0.03%	0.13%
Spar	20,000	Nacelle	-0.06%	0.06%
Spar	40,000	Nacelle	-0.14%	0.15%
Spar (R = 3)	100,000	Platform	0.69%	1.17%
Spar (R = 3)	200,000	Platform	1.33%	2.14%
Spar (R = 3)	400,000	Platform	2.59%	3.85%
Spar (R = 6)	100,000	Platform	0.77%	1.27%
Spar (R = 6)	200,000	Platform	1.57%	2.45%
Spar (R = 6)	400,000	Platform	3.58%	5.02%

Table 8.13: Table showing summary of motion reduction results when using non-uniform TLCD with external forcing method

As shown in Table 8.13, the attachment of a TLCD to each turbine model provides tower top and platform motion reduction in all cases with the exception of the spar nacelle. Though the TLCD provides system motion reduction in most cases, it must be determined as to whether the attachment, operation and maintenance of a TLCD would reduce the overall cost of energy of each of the system.

8.6 Comparison to Ideal TMD

Table 8.14 shows comparisons between the optimization results for each simulated TLCD-coupled OWT when subjected to the external forcing method and the ideal TMD properties (where applicable) derived by Stewart. The TLCDs used are non-

uniform. The values displayed for the spar buoy used are those generated when the radius of the platform has a value of 3 m, similar to the value used in Stewart's simulations.

OWT	TMD/TLCD Mass (kg)	Location	$k_{eq,TLCD}$ (N/m)	k_{tmd} (N/m)	ω_{TLCD} (Hz)	ω_{TMD} (Hz)	$d_{eq,TLCD}$ (Ns/m)	d_{TMD} (Ns/m)
Monopile	10,000	Nacelle	19,130	28,800	1.38	1.70	264,300	2,800
Monopile	20,000	Nacelle	38,090	54,270	1.38	1.65	525,900	7,414
Monopile	40,000	Nacelle	72,170	98,640	1.34	1.57	858,200	19,690
Barge	10,000	Nacelle	2,165	1,237	0.47	0.35	58,980	255
Barge	20,000	Nacelle	4,343	2,345	0.47	0.34	197,200	1,235
Barge	40,000	Nacelle	8,776	5,274	0.47	0.36	298,500	10,183
Barge	100,000	Platform	22,420	-	0.47	-	46,140	-
Barge	200,000	Platform	44,160	-	0.47	-	7,884	-
Barge	400,000	Platform	91,340	-	0.48	-	275,000	-
Spar	10,000	Nacelle	13,760	54,150	1.17	2.33	6,247,000	3,759
Spar	20,000	Nacelle	7,230	10,1430	0.60	2.25	9,145,000	10,076
Spar	40,000	Nacelle	15,500	183,600	0.62	2.14	1,326,000	26,747
Spar	100,000	Platform	121,000	157	0.18	0.04	36,470,000	57,395
Spar	200,000	Platform	129,200	440	0.13	0.05	5,698,000	92,506
Spar	400,000	Platform	193,800	262,100	0.11	0.81	17,750,000	131,008

Table 8.14: Table showing comparisons between optimized TLCD and TMD parameters

Many conclusions can be made by looking at the table. Examining the stiffness values, $k_{eq,TLCD}$ and k_{tmd} are relatively similar for cases involving the monopile and the barge. This causes the natural frequencies of each TLCD in the monopile and barge systems to be similar. The TLCD natural frequencies produced by each OWT system are relatively constant with increasing mass. This shows that the damper system is attempting to damp out a certain natural frequency of the OWT. The differences in values between the TLCD and TMD are attributed to the differences between the TLCD simulation approach used and how FAST models a wind turbine with a TMD as well as constraints set by the nacelle and barge dimensions.

For the values of $k_{eq,TLCD}$ in the spar buoy platform, the values seem to increase in a trend that is consistent with the increase in m_{TLCD}. Spar buoy simulations with the

TLCD in the nacelle produce results that are not entirely consistent. The results show no trends as m_{TLCD} increases. The main factor in determining $k_{eq,TLCD}$ as well as ω_{TLCD} is the L_{ee} term. The value of L_{ee} may be optimized within the given constraints but due to the low natural frequency of the spar and the constraints imposed by the nacelle and spar when placing the TLCD, L_{ee} is not able to reach a value where it can define a ω_{TLCD} that will be effective in reducing spar platform motion.

With regards to the damping values, it is also previously noted that Stewart implemented stops in his model. These stops restrict motion of the TMD and are used to prevent the TMD from exceeding space requirements within the nacelle and platforms. The stops make the TMD system highly non-linear and create some discrepancies between the two models. The TLCD model does not use stops. The TLCD water motion is limited so as not to exceed a certain value for the given defined conditions. Therefore, the TLCD must be able to provide much higher damping to prevent this motion. This is going to generate $d_{eq,TLCD}$ values that are much larger than d_{TMD}. For the monopile and barge, $d_{eq,TLCD}$ increases as m_{TLCD} increases. The equivalent damping for the spar is much more random. As shown in the optimizations for the spar, the optimized values of ζ have no trends or are not grouped together like for the monopile and barge. This is due to the small values of the water motion within the TLCD. The spar's overall low displacement and velocity values keep the water inside the TLCD from oscillating to high levels. The small velocity values make the value of ζ have much less of a contribution to the overall damping of the system. The vibration reduction is much more dependent on the dimension sizes of the TLCD. This causes the value of ζ to not be as consistent as with the monopile or barge, generating more random-like values. Also, the values of L_{ee} have

an impact on the TLCD equivalent damping. Since the TLCD was not as effective in the spar due to the size constraints, the optimization routine struggled to find dimension values that would produce positive results within the constraints. L_{ee} is another term that defines $d_{eq,TLCD}$ and its varying values led the equivalent damping to vary widely for each spar buoy case.

CHAPTER 9

CONCLUSIONS AND FUTURE WORK

The TLCD is an effective type of damper system used for reducing vibrations in civil structures. It is shown that applying a TLCD to a structure such as an OWT can effectively reduce the overall motion of the structure in most scenarios, though some exacerbate the motion. The following objectives are completed within this thesis.

- A methodology is generated to simulate a TLCD-OWT system. EOMs are derived for a limited DOF system for three different OWT configurations, which include various locations for the TLCD. Through the use of a deterministic sweep optimization routine, dimensions are generated for the TLCD. Simulations are successfully performed to output the motion of the TLCD-OWT coupled system in the time domain and the realistic motion of the OWT can be observed.
- Results show that optimally sized TLCDs (within defined constraints) can potentially reduce the vibration of an OWT. It is also shown that the use of an optimized TLCD sometimes provides no benefit to the structural motion of a system. When a TLCD is utilized in an OWT and the results are favorable based on the analysis presented in this thesis, increased fatigue life of the wind turbine and support structure as well as reduced overall cost of energy can potentially be achieved.
- Results show that using a non-uniform cross-sectional area TLCD typically outperform one with a uniform cross-sectional area by shortening the TLCD's length requirement.
- Quantitative comparisons are also made with an optimal TMD. It is shown that optimized TLCDs and TMDs have approximately the same equivalent spring values

and natural frequencies for the monopile and barge, as they work to reduce a particular frequency of the OWT, but vary widely for the spar. TLCDs also have much higher damping values based on the constraints of the modeling analysis compared to the use of a TMD with defined stops.

9.1 Future Research

9.1.1 Applying FAST-SC

The research performed in this thesis needs to be verified using a higher fidelity model. Using FAST-SC, it will be possible to verify that the method outlined in this thesis for finding optimum vibration reduction values of a TLCD-coupled system is accurate. The equations of motion of a TLCD system need to be incorporated into FAST-SC. Proper coding will need to be done so that it can recognize a TLCD and simulate its use in an OWT.

9.1.2 Semi-Active TLCDs

Though the use of an active TLCD was not considered in this thesis, it would be interesting to see how a TLCD with a semi-active component could potentially increase vibration reduction. Much work has been performed for analyzing the use and effectiveness of a semi-active TLCD [32]. A semi-active component would include a controllable valve that would replace the TLCD's orifice, which could be opened or closed to control damping values. Energy does not need to be introduced to the system, but rather the system is designed so that it's able to manipulate system properties to adjust to changing conditions. Altering the damping semi-actively has been shown to

increase system vibration reduction capabilities, and would be an interesting topic for application to the research presented in this thesis.

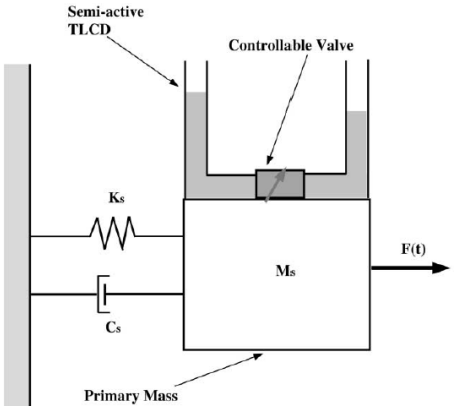

Figure 9.1: Semi-active TLCD used in translating structure system [32]

9.1.3 Cost and Material Analysis

Another topic that must be covered is a cost and material analysis of the TLCD. The vibration experienced by the tower and platform could be used to define cyclic fatigue in the OWT's support structures and it has been concluded that TLCDs reduce the overall motion of an OWT system. Therefore, a TLCD may be effective in reducing overall fatigue of the OWT, especially in its support structures including the tower and platform. This could result in the necessity for less structural material (thinner steel in the tower) or a reduced level of system maintenance.

Though TLCDs may be effective when used in most scenarios, it must be determined as to whether their installation, operation and maintenance are effective at reducing the overall cost of energy of the system. The possible savings achieved in turbine and support structure materials, operation and maintenance would have to outweigh the cost of the installation and maintenance of a TLCD. A study would need to

be done to determine how the TLCD reduces the cyclic loading of the system and how this would translate into possible cost savings. This study would show how the use of a TLCD can affect the overall cost of energy while helping to determine how the use of a TLCD would impact the fatigue life of to OWT tower, platform and related support systems.

APPENDIX A

TLCD-OWT SIMULATION INTERFACE CODE

```
% Program for simulating TLCD-OWT models

% Defined constants
g = 9.81;       % Acceleration due to gravity [m/s^2]
rho = 1000;     % Density of water [kg/m^3]
% TLCD dimensions. Variables defined by user
m_tlcd = 10000; % TLCD mass [kg]
alpha =  1;     % A/A1 vertical/horizontal cross-sectional area [unitless]
B = 10;         % TLCD horizontal length [m]
L = 20;         % TLCD total length [m]
Zeta = 100;     % TLCD damping coefficient [unitless]

% Switches for Platform Type and TLCD location
% Platform Type
platform = 1;   % 1: Barge, 2: Spar, 3: Monopile
% Platform Type and Location of TLCD
P_tlcd = 2;     % 1: Monopile Nacelle, 2: Barge Nacelle, 3: Barge Platform, 4:
                  Spar Nacelle, 5: Spar Platform
%% Barge
if platform ==1
    % Platform
    I_p = 1.76667e9;        % Barge platform inertia [kg-m^2]
    m_p = 5452000;          % Barge platform mass [kg]
    k_p = 1.888e9;          % Barge platform stiffness [N/m]
    d_p = 1.5e9;            % Barge platform damping [N-s/m]
    R_p = 0.281;            % Distance to platform COM below hinge [m]
    % Tower
    I_t = 3.3428e9;         % Barge tower inertia [kg-m^2]
    m_t = 697460;           % Barge tower mass (includes RNA mass) [kg]
    k_t = 1.2519e10;        % Barge tower stiffness [N/m]
    d_t = 6.569e7;          % Barge tower damping [N-s/m]
    R_t = 64.2;             % Distance to tower COM from hinge [m]
    R_rot = 90;             % Distance to rotor from hinge [m]
    height_t = 87.6;        % Distance to tower top from hinge [m]
    % TLCD Location
    if P_tlcd == 2          % TLCD is located in nacelle
        R_tlcd = 90.6;      % Distance to TLCD COM from hinge when TLCD is in
                              nacelle [m]
    elseif P_tlcd == 3      % TLCD is located in platform
        R_tlcd = -10.0;     % Distance to TLCD COM from hinge when TLCD is in
                               platform [m]
    else
        R_tlcd = 0;         % No TLCD present
    end
    % Inputs
    input_p = 5*pi/180;     % Defined platform displacement for Initial
                               Perturbation Method [deg]
%% Spar Buoy
elseif platform ==2
    % Platform
    I_p = 1.1688e11;        % Spar platform inertia [kg-m^2]
    m_p = 7466330;          % Spar platform mass [kg]
    k_p = -5.30e9;          % Spar platform stiffness [N/m]
    d_p = 1.1930e9;         % Spar platform damping [N-s/m]
    R_p = 99.9155;          % Distance to platform COM below hinge [m]
```

```
    % Tower
    I_t = 2.5186e9;          % Spar tower inertia [kg-m^2]
    m_t = 599718;            % Spar tower mass (includes RNA mass) [kg]
    k_t = 1.42e10;           % Spar tower stiffness [N/m]
    d_t = 1.2e9;             % Spar tower damping [N-s/m]
    R_t = 60.5961;           % Distance to tower COM from hinge [m]
    R_rot = 80;              % Distance to rotor from hinge [m]
    height_t = 77.6;         % Distance to tower top from hinge [m]
    R = 3;                   % Spar radius [m]
    % TLCD
    if P_tlcd == 4           % TLCD is located in nacelle
        R_tlcd = 80.6;       % Distance to TLCD COM from hinge when TLCD is in
                               nacelle [m]
    elseif P_tlcd == 5       % TLCD is located in platform
        R_tlcd = -118;       % Distance to TLCD COM from hinge when TLCD is in
                               platform [m]
    else
        R_tlcd = 0;          % No TLCD present
    end
    % Inputs
    input_p = 5*pi/180;      % Defined platform displacement for Initial
                               Perturbation Method [deg]
%% Monopile
elseif platform ==3 && P_tlcd == 1
    % Tower
    I_t = 3.3428e9;             % Monopile tower inertia [kg-m^2]
    m_t = 697460;               % Monopile tower mass (includes RNA mass) [kg]
    k_t = 1.0519e10;            % Monopile tower stiffness [N/m]
    d_t = 1.1e9;                % Monopile tower damping [N-s/m]
    R_t = 64.2;                 % Distance to tower COM from hinge [m]
    R_rot = 90;                 % Distance to rotor from hinge [m]
    height_t = 87.6;            % Distance to tower top from hinge [m]
    % TLCD
    R_tlcd = 90.6;              % Distance to TLCD COM from hinge when TLCD is
                                  in nacelle [m]
    %Inputs
    input_t = (1.4/height_t);   % Defined tower top displacement for Initial
                                  Perturbation Method [m]
end

%%
% User defines OWT, TLCD location and simulation method using "force_flag"
% See Appendix B for example of external file that contains equations of motion
% of the system

force_flag = 3;     % 1: Monopile Pert, 2: Monopile Ext.Force, 3: Barge Nacelle
                      Pert, 4: Barge Nacelle Ext.Force 5: Barge Platform Pert,
                      6: Barge Platform Ext.Force, 7: Spar Nacelle Pert, 8:
                      Spar Nacelle Ext.Force, 9: Spar Platform Pert, 10: Spar
                      Platform Ext.Force

    % Dependent TLCD variables
    Lee = L - B+ alpha*B;               % Length of equivalent uniform liquid
                                          column with cross-sectional area A
                                          that possesses the same energy as the
                                          TLCD [m]
    omega_l = sqrt((2*g)/Lee)/(2*pi);   % TLCD natural frequency [Hz]
    H = (L-B)/2;                        % Height of TLCD vertical column [m]
    A = m_tlcd/(rho*((B/alpha)+(L-B))); % Vertical column cross-sectional area
                                          [m^2]
    A1 = A/alpha;                       % Horizontal column cross-sectional
                                          area [m^2]
```

```
% Comments apply similarly to each section for Initial Perturbation method and
External Forcing Method

% Monopile Nacelle
if force_flag == 1 % Initial Perturbation Method
    dt = .125;                  % Time step [s]
    t_span = [0:dt:100]';       % Simulation time span [s]
    thrust = 500000;            % Constant aerodynamic thrust value [N]
    y0 = [input_t 0 0 0 0 0]';  % Initial conditions
    [t_out,y_out] = ode45(@(t,y) Mono_Pert(t, y, A, A1, alpha, B, Lee, Zeta,
       rho, g, m_tlcd, R_tlcd, m_t, I_t, k_t, d_t, R_t, thrust,
       R_rot),t_span,y0);       % References external file that contains
                                   equations of motion of the system
elseif force_flag == 2 % External Forcing Method
    dt = .125;                  % Time step [s]
    load T_syn;                 % Loads synthesized aerodynamic thrust
    ind = find(t_syn==300);     % Defines a 300 second simulation time interval
    t_span = t_syn(1:ind,1);    % Simulation time span [s]
    T = T_syn(1:ind,1);         % Aerodynamic thrust value for each time step
                                   [N]
    My = T*R_rot;               % Aerodynamic moment imposed on tower [N-m]
    y0 = [0 0 0 0 0 0]';        % Initial conditions
    [t_out,y_out] = ode45(@(t,y) Mono_Thrust(t, y, A, A1, alpha, B, Lee, Zeta,
       rho, g, m_tlcd, R_tlcd, m_t, I_t, k_t, d_t, R_t, My, t_span,
       dt),t_span,y0); % References external file that contains equations of
                          motion of the system (See Appendix B)
% Barge Nacelle
elseif force_flag == 3 % Initial Perturbation Method
    dt = .125;
    t_span = [0:dt:100]';
    thrust = 500000;
    y0 = [0 0 0 0 input_p 0]';
    [t_out,y_out] = ode45(@(t,y) Barge_Nacelle_Pert(t, y, A, A1, alpha, B, Lee,
       Zeta, rho, g, m_tlcd, R_tlcd, m_t, I_t, k_t, d_t, R_t, I_p, d_p, k_p,
       m_p, R_p, thrust, R_rot),t_span,y0);
elseif force_flag == 4 % External Forcing Method
    dt = .125;
    load MP_syn;            % Loads synthesized hydrodynamic pitching moment
    load T_syn              % Loads synthesized aerodynamic thrust
    ind = find(t_syn==300);
    t_span = t_syn(1:ind,1);
    MP = MP_syn(1:ind,1);   % Hydrodynamic pitching moment value for each time
                               step [N-m]
    T = T_syn(1:ind,1);
    My = T*R_rot;
    y0 = [0 0 0 0 0 0]';
    [t_out,y_out] = ode45(@(t,y) Barge_Nacelle_Pitch(t, y, A, A1, alpha, B,
       Lee, Zeta, rho, g, m_tlcd, R_tlcd, m_t, I_t, k_t, d_t, R_t, I_p, d_p,
       k_p, m_p, R_p, MP, My, t_span, dt),t_span,y0); % See Appendix B
%Barge Platform
elseif force_flag == 5 % Initial Perturbation Method
    dt = .125;
    t_span = [0:dt:100]';
    thrust = 500000;
    y0 = [0 0 0 0 input_p 0]';
    [t_out,y_out] = ode45(@(t,y) Barge_Platform_Pert(t, y, A, A1, alpha, B,
       Lee, Zeta, rho, g, m_tlcd, R_tlcd, m_t, I_t, k_t, d_t, R_t, I_p, d_p,
       k_p, m_p, R_p, thrust, R_rot),t_span,y0);
elseif force_flag == 6 % External Forcing Method
    dt = .125;
    load MP_syn;
    load T_syn
    ind = find(t_syn==300);
```

```
    t_span = t_syn(1:ind,1);
    MP = MP_syn(1:ind,1);
    T = T_syn(1:ind,1);
    My = T*R_rot;
    y0 = [0 0 0 0 0 0]';
    [t_out,y_out] = ode45(@(t,y) Barge_Platform_Pitch(t, y, A, A1, alpha, B,
       Lee, Zeta, rho, g, m_tlcd, R_tlcd, m_t, I_p, d_p, k_p, m_p, R_p, I_t,
       k_t, d_t, R_t, MP, My, t_span, dt),t_span,y0);
%Spar Nacelle
elseif force_flag == 7 % Initial Perturbation Method
    dt = .125;
    t_span = [0:dt:100]';
    thrust = 500000;
    y0 = [0 0 0 0 input_p 0]';
    [t_out,y_out] = ode45(@(t,y) Spar_Nacelle_Pert(t, y, A, A1, alpha, B, Lee,
       Zeta, rho, g, m_tlcd, R_tlcd, m_t, I_t, k_t, d_t, R_t, I_p, d_p, k_p,
       m_p, R_p, thrust, R_rot),t_span,y0);
elseif force_flag == 8 % External Forcing Method
    dt = .125;
    load MP_spar;
    load T_syn
    ind = find(t_syn==300);
    t_span = t_syn(1:ind,1);
    MP = MP_spar(1:ind,1);
    T = T_syn(1:ind,1);
    My = T*R_rot;
    y0 = [0 0 0 0 0 0]';
    [t_out,y_out] = ode45(@(t,y) Spar_Nacelle_Thrust(t, y, A, A1, alpha, B,
       Lee, Zeta, rho, g, m_tlcd, R_tlcd, m_t, I_t, k_t, d_t, R_t, I_p, d_p,
       k_p, m_p, R_p, MP, My, t_span, dt),t_span,y0);
%Spar Platform
elseif force_flag == 9 % Initial Perturbation Method
    dt = .125;
    t_span = [0:dt:100]';
    thrust = 500000;
    y0 = [0 0 0 0 input_p 0]';
    [t_out,y_out] = ode45(@(t,y) Spar_Platform_Pert(t, y, A, A1, alpha, B, Lee,
       Zeta, rho, g, m_tlcd, R_tlcd, m_t, I_t, k_t, d_t, R_t, I_p, d_p, k_p,
       m_p, R_p, thrust, R_rot),t_span,y0);
elseif force_flag == 10 % External Forcing Method
    dt = .125;
    load MP_spar;
    load T_syn
    ind = find(t_syn==300);
    t_span = t_syn(1:ind,1);
    MP = MP_spar(1:ind,1);
    T = T_syn(1:ind,1);
    My = T*R_rot;
    y0 = [0 0 0 0 0 0]';
    [t_out,y_out] = ode45(@(t,y) Spar_Platform_Thrust(t, y, A, A1, alpha, B,
       Lee, Zeta, rho, g, m_tlcd, R_tlcd, m_t, I_t, k_t, d_t, R_t, I_p, d_p,
       k_p, m_p, R_p, MP, My, t_span, dt),t_span,y0);
end

% System motion outputs
ttd = height_t*(y_out(:,1));                % Time series output of TTD
StDev_TTD = std(ttd);                       % Standard deviation of TTD
W_disp = (y_out(:,3));                      % Time series output of wDisp
StDev_Wdisp = std(W_disp);                  % Standard deviation of wDisp
Platform_Pitch = (y_out(:,5)*180/pi);       % Time series output of PlatPitch
StDev_Platform_Pitch = std(Platform_Pitch); % Standard deviation of PlatPitch

% Plotting time series of outputs
```

```
subplot(3,1,1)
plot(t_out, Platform_Pitch)
title('Platform Pitch')
xlabel('Time [s]')
ylabel('Pitch [deg]')
subplot(3,1,2)
plot(t_out, ttd)
title('Tower Top Displacement')
xlabel('Time [s]')
ylabel('TTD [m]')
subplot(3,1,3)
plot(t_out, (y_out(:,3)))
title('TLCD Water Displacement')
xlabel('Time [s]')
ylabel('Water Displacement [m]')

% Display tabular output of parameter values
Results = zeros(1,10);
    Results(1,1) = A;
    Results(1,2) = A1;
    Results(1,3) = alpha;
    Results(1,4) = B;
    Results(1,5) = L;
    Results(1,6) = Lee;
    Results(1,7) = Zeta;
    Results(1,8) = StDev_TTD;
    Results(1,9) = StDev_Wdisp;
    Results(1,10) = StDev_Platform_Pitch;
disp('All TLCD/Motion Data')
disp(Results);
```

APPENDIX B

EXAMPLE EQUATIONS OF MOTION CODE

```
% Example showing External Forcing Method with equations of motion of the barge
      with TLCD in nacelle

function dy = Barge_Nacelle_Pitch(t, y, A, A1, alpha, B, Lee, Zeta, rho, g,
              m_tlcd, R_tlcd, m_t, I_t, k_t, d_t, R_t, I_p, d_p, k_p, m_p, R_p,
              MP, My, t_span, dt)

Pitching_moment = interp1(t_span, MP, t);
Thrust_moment = interp1(t_span, My, t);

% Platform
dy(6,1) = 1/I_p*( -d_p*y(6) - k_p*y(5) - (m_p*g*R_p)*y(5) + k_t*y(1) + d_t*y(2)
      + Pitching_moment);
dy(5,1) = y(6,1);
% Tower
dy(2,1) = (1/(I_t - ((rho*B^2*R_tlcd^2*A1)/Lee) +
      m_tlcd*R_tlcd^2))*((m_t*g*R_t)*(y(1)+y(5)) - I_t*dy(6,1) - k_t*y(1) -
      d_t*y(2) + ((2*rho*A*B*R_tlcd*g)/Lee)*y(3) +
      ((rho*A*B*R_tlcd*Zeta)/(2*Lee))*abs(y(4))*y(4) -
      ((rho*A*B^2*R_tlcd*g)/(alpha*Lee))*(y(1)+y(5)) + (rho*A*g*B)*y(3) +
      Thrust_moment +
      ((1/2)*(8/9)*1.225*pi*63^2*2*10*(90*y(2)+90.281*y(6))*dt));
dy(1,1) = y(2,1);
% TLCD
dy(4,1) = (-(2*g)/Lee)*y(3) - (Zeta/(2*Lee))*abs(y(4))*y(4) -
      ((B*R_tlcd)/(alpha*Lee))*(dy(2,1)+dy(6,1)) +
      ((B*A1*g)/(A*Lee))*(y(1)+y(5));
dy(3,1) = y(4,1);
```

BIBLIOGRAPHY

1) Aiken, I.D., Kelly, J.M., 1992, "Comparative study of four passive energy dissipation systems," *NZ National Society of Earthquake Engineering Bulletin*, **25**(3), pp. 175-192.

2) Biswajit, B., Colwell, S., 2009, "Tuned liquid column dampers in offshore wind turbines for structural control*," Journal of Engineering Structures*, **31**, pp. 358-68.

3) Basu, B., Colwell, S., 2007, "Vibration control of an offshore wind turbine with a tuned liquid column damper," Proc. 11th International Conference on Civil, Structural and Environmental Engineering.

4) Butterfield, S., Musial, W., Ram, B., 2006, "Energy from offshore wind," Offshore Technology Conference, Houston, Texas, 2006, Conference Paper No. NREL/CP-500-39450.

5) Butterfield, S., Jonkman, J., Musial, W., Sclavounos, P., 2007, "Engineering Challenges For Floating Offshore Wind Turbines," Offshore Wind Conference, Copenhagen, Denmark, 2005, Conference Paper No. NREL/CP-500-38776.

6) Butterfield, S., Jonkman, J., Musial, W., Scott, G., 2008, "Definition of a 5MW reference wind turbine for offshore system development," Technical Report No. 500-38060, National Renewable Energy Laboratory, Golden, CO.

7) Constantinou, M.C., Symans, M.D., 1993, "Experimental study of seismic response of buildings with supplemental fluid dampers," *Journal of Structural Design Tall Buildings*, **2**(2), pp. 93-132.

8) Dargush, G.F., Soong, T.T., 1997, *Passive energy dissipation systems in structural engineering*, Wiley, London, England, pp. 267.

9) Den Hartog, J.P., 1956, *Mechanical Vibrations: Fourth Edition*, McGraw-Hill Book Company, New York City, New York, pp. 35.

10) Gao, H., Kwok, K.C.S., Samali, B., 1997, "Optimization of tuned liquid column dampers," *Engineering Structures*, **19**(6), pp. 476-86.

11) Gaudiosi, G., Twidell, J., 2009, *Offshore Wind Power*, Brentwood: Multi-Science Pub., Essex, UK, Chap. 2.

12) Hatch, Gareth, 2009, "Why Are Wind Turbines Getting Bigger?," Terra Magnetica & Systems, EWEA 2007, http://www.terramagnetica.com

13) Haskell, G., Lee, D., 2007, "Fluid viscous damping as an alternative to base isolation." Taylor Devices Inc., http://www.thomasnet.com

14) Hengeveld, J., Wilmink, A., 2006, "Application of tuned liquid column dampers in wind turbines," Technical Report, Mecal Applied Mechanics, Netherlands.

15) Housner, G. W. et al., 1997, "Structural control: past, present, and future," *Journal of Engineering Mechanics*, **123**(9), pp. 897-971.

16) Karna, T., Kolari, K., 2004, "Mitigation of dynamic ice actions on offshore wind turbines," Proc. 7th European Conference on Structural Control, pp. 1-4, http://www.karna.eu/pdf/mitigation_of_dynamic_ice.pdf

17) Kwok, K.C.S, Samali, B., Xu, Y.L., 1992, "Control of along wind response of structures by mass and liquid dampers," *Journal of Engineering Mechanics*, **118**(1), pp. 20-39.

18) Lackner, M., Rotea, M., 2010, "Structural control of floating wind turbines," *Mechatronics*, in press, available online.

19) Lin, Y.Y., Shen, Y.C., Shih, M.H., Wu, J.C., 2005, "Design guidelines for tuned liquid column damper for structures responding to wind," *Journal of Engineering Structures*, **27**(13), pp. 1893-1905.

20) Manwell, J. F., McGowan, J.G., Rogers, A.L., 2009, *Wind Energy Explained: Theory, Design and Application, 2nd Edition*, Wiley, Chichester, U.K., pp. 461.

21) National Renewable Energy Laboratory, 2011, "U.S. wind resources and population centers," Map, *Http://www.nauticawindpower.com/offshore_wind/*

22) PDL, 2011, "Design- Pall Friction Dampers," Pall Dynamics Limited, http://www.palldynamics.com.

23) Sakai, F., Takaeda, S., Tamaki, T., 1989, "Tuned liquid column damper – new type device for suppression of building vibrations," Proc. International Conference on Highrise Buildings, pp. 926-931.

24) Stewart, G.M., 2011, "Load reduction of floating wind turbines using tuned mass dampers," Master's thesis, University of Massachusetts Amherst, Amherst, MA.

25) Sain, M.K., Spencer Jr., B.F., 1997, "Controlling buildings: a new frontier in feedback," *IEEE Control Systems*, pp.19-35.

26) Shinozuka, M., Jan, C.-M., 1972, "Digital simulation of random process and its application," *Journal of Sound and Vibration*, **25**(1), pp. 111-128.

27) Soong, T.T., Spencer Jr., B.F., 2002, "Supplemental energy dissipation: state-of-the-art and state-of-the-practice," *Journal of Engineering Structures*, **24**, pp. 243-259.

28) Taylor Devices India Pvt. Ltd., "Supplementary damping – a new concept in earthquake resistant buildings." General awareness, http://www.taylordevicesindia.com/D_Aware_PDF/07SupplementaryDampingANewConceptinEarthquakeResistantBuildings.pdf

29) Watkins, R.D., 1991, "Tests on a liquid column vibration absorber for tall structures," Proc. Int. Conf. on Steel and Aluminum Structures, Singapore.

30) Watkins, R.D., Hitchcock, P.A., 1992, "Tests on various liquid column vibration absorbers," Proc. Int. Conf. on Motion and Vibration Control, Yokohama, Japan, pp. 1130-1134.

31) Wei, 2007, "Damper Baby," http://www.flickr.com/photos/weilei/578087864/

32) Yalla, S.K., Kareem, A., 2000, "Optimal absorber parameters for tuned liquid column dampers," Journal of Structural Engineering, 126(8), pp. 906-15.

33) Yao, J.T.P., 1972, "Concept of structural control," *Journal of Structural Engineering*, **98**, pp. 1567-1574.

34) Ziegler, F., 2007, "The tuned liquid column damper as the cost-effective alternative of the mechanical damper in civil engineering structures," *International Journal of Acoustics and Vibration*, **12**(1), pp.25-39.